Ag I and Pb II as Additional Assembling Cations in Uranyl Coordination Polymers and Frameworks

Pierre Thuéry, Jack Harrowfield

Ag^{I} and Pb^{II} as Additional Assembling Cations in Uranyl Coordination Polymers and Frameworks

Pierre Thuéry*,† and Jack Harrowfield*,‡

†NIMBE, CEA, CNRS, Université Paris-Saclay, CEA Saclay, 91191 Gif-sur-Yvette, France

‡ISIS, Université de Strasbourg, 8 allée Gaspard Monge, 67083 Strasbourg, France

ABSTRACT: Five mono- or polycarboxylic acids have been used to generate a series of eight heterometallic uranyl complexes involving silver(I) or lead(II) cations, all synthesized under (solvo)-hydrothermal conditions. Pimelic acid (H_2pim) gave complexes $[Ag(bipy)_2]_2[UO_2(pim)(NO_3)]_2$ (**1**) and $[UO_2Pb(pim)_2(bipy)(H_2O)]\cdot0.5bipy\cdot H_2O$ (**2**) (bipy = 2,2′-bipyridine), which both crystallize as one-dimensional (1D) polymers, but differ in that the silver(I) cations are separate counter-ions, while carboxylate-bound lead(II) cations are an essential component of the polymer. Only silver(I)-containing species were obtained with all-*cis* 1,3,5-cyclohexanetricarboxylic acid (H_3chtc), $[UO_2Ag(chtc)(H_2O)_2]$ (**3**) and $[Ag(bipy)(CH_3CN)]_2[UO_2(chtc)]_2$ (**4**); both contain two-dimensional (2D) uranyl carboxylate subunits with honeycomb $\{6^3\}$ topology, these being united into a three-dimensional (3D) framework with the lonsdaleite $\{6^6\}$ topology by bridging, oxo-bound silver(I) cations in **3**. Both silver- and lead-containing complexes were obtained with 3,3′,4,4′-biphenyltetracarboxylic acid (H_4bptc), $[UO_2Ag(bptc)(4,4'\text{-bipyH})]$ (**5**) and $[UO_2Pb(bptc)(bipy)_2]$ (**6**) (4,4′-bipy = 4,4′-bipyridine), and they both display a 2D uranyl carboxylate network with the $\{4^4.6^2\}$ topology, the additional cations and *N*-donors being decorating species. In this case, a higher dimensionality was obtained not with an additional cation, but with a coordinated *N*-methyl-2-pyrrolidone (NMP) molecule, since $[(UO_2)_2(bptc)(NMP)_{1.5}(H_2O)_{1.5}]\cdot1.5H_2O$ (**7**) crystallizes as a three-dimensional (3D) framework. In the presence of silver(I), 3-pyrimidin-2-yl-benzoic acid (Hpyb) gave the complex $[UO_2Ag(pyb)_3(H_2O)_2]\cdot4H_2O$ (**8**), in which the two coordination sites are occupied in accord with Hard/Soft Acid/Base (HSAB) principles, uranyl being chelated by three carboxylate groups and silver(I) being bound to nitrogen atoms; the 1D polymer formed bridges to another through silver–uranyl oxo bonding. In contrast, the homometallic, molecular complex $[UO_2(pyb)_2(bipy)]$ (**9**) was obtained in the presence of lead(II) cations. The lead-containing complex with 2,6-pyridinedicarboxylic acid (H_2pydc), $[UO_2Pb_2(pydc)_2(phen)_2(HCOO)_{1.5}(NO_3)_{0.5}]\cdot0.5H_2O$ (**10**) (phen = 1,10-phenanthroline), crystallizes as a 1D polymer in which uranyl is bound to two *O*,*N*,*O*-donors, as usual with this ligand, polymerization being due to lateral double lead(II) bridges. Variations in uranyl emission maxima positions appear to be essentially related to the uranium coordination number within the present series.

INTRODUCTION

Association of uranyl ions with other cations, particularly d-block but also alkali metal, alkaline-earth metal and lanthanide species, is a widespread strategy to increase the dimensionality in uranyl–organic coordination polymers,[1–3] either through additional bridges involving the ligands, or through direct bonding to uranyl oxo groups, or both.[4,5] Even incorporation of the second metal cation as an isolated counter-ion offers many possibilities for modulating the dimensionality and geometry of the uranyl-containing polymer.[5–9] In contrast to the d-block metal cations most often used in the synthesis of such complexes, which are cations typically displaying octahedral coordination geometry (suitable in particular for generating chiral counter-ions with three chelating *N*-donors), silver(I), which is found in uranyl-based systems containing carboxylate[10–18] or phosphonate[19–22] ligands, is noteworthy for its diverse coordination modes, with coordination numbers as low as 3 or even 2,[23] and including binding to carbon donors.[17] The occurrence of argentophilic interactions[24] may result in peculiar arrangements of the counter-ions, columnar for example, that themselves may induce novel architectures of the anionic uranyl-containing polymer.[15] Another metallic cation displaying irregular coordination geometries and highly variable coordination numbers, ranging from 2 to 10, is lead(II), which has not often been used in association with uranyl cations.[11,17,18,25] The possible but controversial effects of lead(II) lone pair on its coordination preferences[26–30] adds further interest to such a study. The reported uranyl–silver(I) complexes with carboxylate ligands involve acetate,[12] pimelate,[16] benzene-1,4-dicarboxylate,[10] 1,3,5-benzenetriacetate,[17] 1,4-naphthalenedicarboxylate,[13] isonicotinate,[14] 2,6-pyridinedicarboxylate,[11] tetrahydrofurantetracarboxylate,[18] and 2,5-thiophenedicarboxylate,[15] while known uranyl–lead(II) species contain acetate,[25] 2,6-pyridinedicarboxylate,[11] 1,3,5-benzenetriacetate,[17] and tetrahydrofurantetracarboxylate,[18] these four ligands being thus

represented in both series. As we and others[10–18,25] have shown, Ag^{I} and Pb^{II} in various additionally complexed forms can compete with uranyl ion for such ligands in very different ways, thus engendering quite different structures for the coordination polymers formed with any one ligand. In order to further investigate the effect of the presence of Ag^{I} or Pb^{II} on the formation of uranyl–organic coordination polymers, as well as the possibly associated increase in dimensionality leading to frameworks, we have conducted a study involving several mono- or polycarboxylates differing greatly from one another in order to explore a particularly broad range of structural possibilities. We report here the synthesis, crystal structure determination and, in most cases, uranyl emission properties of a series of heterometallic complexes obtained from pimelic (H_2pim), all-*cis*-1,3,5-cyclohexanetricarboxylic (H_3chtc), 3,3′,4,4′-biphenyltetracarboxylic (H_4bptc), 3-pyrimidin-2-yl-benzoic (Hpyb) and 2,6-pyridinedicarboxylic (H_2pydc) acids. In some instances, both silver(I)- and lead(II)-containing species could be obtained, while in others only one of them could be crystallized; two homometallic uranyl complexes are also reported for comparison purposes. Some of these ligands, such as H_2pim[16,31–35] and H_2pydc,[11,36–45] have been frequently used in uranyl structural chemistry while H_3chtc,[46] H_4bptc[47] and Hpyb[48] are more unusual. Although a dimensionality increase leading to formation of a three-dimensional (3D) framework and clearly attributable to the presence of silver(I) cations occurs in only one case, several complexes in this series display original features (among which Ag^{I} or Pb^{II} oxo-bonding to uranyl). Uranyl emission in the solid state has also been investigated in most cases and reveals a correlation between maxima positions and uranium coordination number more clearcut than usually found.

EXPERIMENTAL SECTION

Syntheses. Caution! *Uranium is a radioactive and chemically toxic element, and uranium-containing samples must be handled with suitable care and protection.*

$UO_2(NO_3)_2 \cdot 6H_2O$ (depleted uranium, R. P. Normapur, 99%), $AgNO_3$ and $Pb(NO_3)_2$ were purchased from Prolabo, 2,2′-bipyridine (bipy) and 4,4′-bipyridine (4,4′-bipy) were from Fluka, and pimelic acid (H_2pim), all-*cis* 1,3,5-cyclohexanetricarboxylic acid (H_3chtc), 3,3′,4,4′-biphenyltetracarboxylic acid dianhydride, 3-pyrimidin-2-yl-benzoic acid (Hpyb), 2,6-pyridinedicarboxylic acid (H_2pydc), and 1,10-phenanthroline (phen) were from Aldrich. Elemental analyses were performed by MEDAC Ltd. at Chobham, UK.

$[Ag(bipy)_2]_2[UO_2(pim)(NO_3)]_2$ ***(1)***. Pimelic acid (16 mg, 0.10 mmol), $UO_2(NO_3)_2 \cdot 6H_2O$ (50 mg, 0.10 mmol), $AgNO_3$ (34 mg, 0.20 mmol), 2,2′-bipyridine (32 mg, 0.20 mmol), methanol (0.2 mL), and demineralized water (0.6 mL) were placed in a 15 mL tightly closed glass vessel and heated at 140 °C under autogenous pressure, giving light yellow crystals of complex **1** within three days (17 mg, 19% yield based on U). Anal. calcd for $C_{54}H_{52}Ag_2N_{10}O_{18}U_2$: C, 35.62; H, 2.88; N, 7.69. Found: C, 35.72; H, 2.72; N, 7.72%.

$[UO_2Pb(pim)_2(bipy)(H_2O)] \cdot 0.5bipy \cdot H_2O$ ***(2)***. Pimelic acid (16 mg, 0.10 mmol), $UO_2(NO_3)_2 \cdot 6H_2O$ (25 mg, 0.05 mmol), $Pb(NO_3)_2$ (17 mg, 0.05 mmol), 2,2′-bipyridine (16 mg, 0.10 mmol), *N*,*N*-dimethylformamide (0.2 mL), and demineralized water (0.8 mL) were placed in a 15 mL tightly closed glass vessel and heated at 140 °C under autogenous pressure, giving light yellow crystals of complex **2** within three days (15 mg, 28% yield). Anal. calcd for $C_{29}H_{36}N_3O_{12}PbU$: C, 32.74; H, 3.41; N, 3.95. Found: C, 32.33; H, 3.28; N, 3.91%.

$[UO_2Ag(chtc)(H_2O)_2]$ ***(3)***. 1,3,5-Cyclohexanetricarboxylic acid (11 mg, 0.05 mmol), $UO_2(NO_3)_2 \cdot 6H_2O$ (25 mg, 0.05 mmol), $AgNO_3$ (17 mg, 0.10 mmol), and demineralized water (0.7 mL) were placed in a 15 mL tightly closed glass vessel and heated at 140 °C under autogenous pressure, giving light yellow crystals of complex **3** within three days (9 mg, 29% yield). Anal. calcd for $C_9H_{13}AgO_{10}U$: C, 17.24; H, 2.09. Found: C, 17.32; H, 2.01%.

[Ag(bipy)(CH$_3$CN)]$_2$[UO$_2$(chtc)]$_2$ ***(4)***. 1,3,5-Cyclohexanetricarboxylic acid (22 mg, 0.10 mmol), $UO_2(NO_3)_2 \cdot 6H_2O$ (50 mg, 0.10 mmol), $AgNO_3$ (17 mg, 0.10 mmol), 2,2′-bipyridine (16 mg, 0.10 mmol), acetonitrile (0.2 mL), and demineralized water (0.8 mL) were placed in a 15 mL tightly closed glass vessel and heated at 140 °C under autogenous pressure, giving light yellow crystals of complex **4** overnight (33 mg, 42% yield). Anal. calcd for $C_{21}H_{20}AgN_3O_8U$: C, 32.00; H, 2.56; N, 5.33. Found: C, 32.10; H, 2.70; N, 5.32%.

[UO$_2$Ag(bptc)(4,4′-bipyH)] ***(5)***. 3,3′,4,4′-Biphenyltetracarboxylic acid dianhydride (30 mg, 0.10 mmol), $UO_2(NO_3)_2 \cdot 6H_2O$ (50 mg, 0.10 mmol), $AgNO_3$ (17 mg, 0.10 mmol), 4,4′-bipyridine (16 mg, 0.10 mmol), acetonitrile (0.2 mL), and demineralized water (0.8 mL) were placed in a 15 mL tightly closed glass vessel and heated at 140 °C under autogenous pressure, giving light yellow crystals of complex **5** within one month (21 mg, 24% yield). Elemental analysis results are consistent with the additional presence of about one water molecule probably resulting from hydration of the powdered sample before analysis. Anal. calcd for $C_{26}H_{15}AgN_2O_{10}U + H_2O$: C, 35.52; H, 1.95; N, 3.19. Found: C, 35.37; H, 1.95; N, 3.00%.

[UO$_2$Pb(bptc)(bipy)$_2$] ***(6)***. 3,3′,4,4′-Biphenyltetracarboxylic acid dianhydride (30 mg, 0.10 mmol), $UO_2(NO_3)_2 \cdot 6H_2O$ (50 mg, 0.10 mmol), $Pb(NO_3)_2$ (33 mg, 0.10 mmol), 2,2′-bipyridine (32 mg, 0.20 mmol), *N*,*N*-dimethylformamide (0.2 mL), and demineralized water (0.8 mL) were placed in a 15 mL tightly closed glass vessel and heated at 140 °C under autogenous pressure, giving light yellow crystals of complex **6** in low yield within one week.

[(UO$_2$)$_2$(bptc)(NMP)$_{1.5}$(H$_2$O)$_{1.5}$]·1.5H$_2$O ***(7)***. 3,3′,4,4′-Biphenyltetracarboxylic acid dianhydride (30 mg, 0.10 mmol), $UO_2(NO_3)_2 \cdot 6H_2O$ (50 mg, 0.10 mmol), *N*-methyl-2-pyrrolidone (0.2 mL), and demineralized water (0.8 mL) were placed in a 15 mL tightly closed glass vessel and

heated at 140 °C under autogenous pressure, giving light yellow crystals of complex **7** in low yield within one month.

*$[UO_2Ag(pyb)_3(H_2O)_2]\cdot 4H_2O$ (**8**).* 3-Pyrimidin-2-yl-benzoic acid (10 mg, 0.05 mmol), $UO_2(NO_3)_2\cdot 6H_2O$ (25 mg, 0.05 mmol), $AgNO_3$ (17 mg, 0.10 mmol), acetonitrile (0.2 mL), and demineralized water (0.5 mL) were placed in a 15 mL tightly closed glass vessel and heated at 140 °C under autogenous pressure, giving light yellow crystals of complex **8** in low yield within one month.

*$[UO_2(pyb)_2(bipy)]$ (**9**).* 3-Pyrimidin-2-yl-benzoic acid (10 mg, 0.05 mmol), $UO_2(NO_3)_2\cdot 6H_2O$ (25 mg, 0.05 mmol), $Pb(NO_3)_2$ (17 mg, 0.05 mmol), 2,2′-bipyridine (16 mg, 0.10 mmol), acetonitrile (0.2 mL), and demineralized water (0.5 mL) were placed in a 15 mL tightly closed glass vessel and heated at 140 °C under autogenous pressure, giving light yellow crystals of complex **9** within three days (15 mg, 73% yield based on the acid). Anal. calcd for $C_{32}H_{22}N_6O_6U$: C, 46.61; H, 2.69; N, 10.19. Found: C, 46.47; H, 2.79; N, 10.15%.

*$[UO_2Pb_2(pydc)_2(phen)_2(HCOO)_{1.5}(NO_3)_{0.5}]\cdot 0.5H_2O$ (**10**).* 2,6-Pyridinedicarboxylic acid (17 mg, 0.10 mmol), $UO_2(NO_3)_2\cdot 6H_2O$ (50 mg, 0.10 mmol), $Pb(NO_3)_2$ (17 mg, 0.05 mmol), 1,10-phenanthroline (18 mg, 0.10 mmol), *N*,*N*-dimethylformamide (0.2 mL), and demineralized water (0.7 mL) were placed in a 15 mL tightly closed glass vessel and heated at 140 °C under autogenous pressure, giving light yellow crystals of complex **10** within three days (5 mg, 13% yield based on lead). Anal. calcd for $C_{39.5}H_{24.5}N_{6.5}O_{15}Pb_2U$: C, 32.00; H, 1.67; N, 6.14. Found: C, 31.95; H, 1.87; N, 6.22%.

Crystallography. The data were collected at 150(2) K on a Nonius Kappa-CCD area detector diffractometer[49] using graphite-monochromated Mo Kα radiation (λ = 0.71073 Å). The

crystals were introduced into glass capillaries with a protective coating of Paratone-N oil (Hampton Research). The unit cell parameters were determined from ten frames, then refined on all data. The data (combinations of φ- and ω-scans with a minimum redundancy of at least 4 for 90% of the reflections) were processed with HKL2000.[50] Absorption effects were corrected empirically with the program SCALEPACK.[50] The structures were solved by intrinsic phasing with SHELXT,[51] except for that of compound **10**, which was solved from Patterson map interpretation; they were then expanded by subsequent difference Fourier synthesis and refined by full-matrix least-squares on F^2 with SHELXL-2014.[52] All non-hydrogen atoms were refined with anisotropic displacement parameters. The hydrogen atoms bound to oxygen or nitrogen atoms were found on difference Fourier maps (except for those of some water molecules in compounds **7**, **8** and **10**) and all the other hydrogen atoms were introduced at calculated positions; all hydrogen atoms were treated as riding atoms with an isotropic displacement parameter equal to 1.2 times that of the parent atom (1.5 for CH_3, with optimized geometry). Special details are as follows:

Compound **1**. Restraints on displacement parameters were applied for the atoms of one bipy molecule probably affected by unresolved disorder.

Compound **3**. The value of the refined Flack parameter was –0.006(3).[53]

Compounds **4** and **9**. Two-component twinning was detected with TwinRotMat[54] and was taken into account in the refinement.

Compound **7**. The NMP molecule containing O14 is very badly resolved and it seemingly occupies the same coordination site as a water molecule. A solvent water molecule (O17) is too close to this NMP molecule and is has been surmised that it was only present when a water molecule was coordinated instead of NMP; all these disordered groups have been given occupancy factors of 0.5. Restraints on some bond lengths, angles and displacement parameters were applied

for the NMP molecules. The highest residual electron density peaks are located near the disordered NMP molecule.

Compound **10**. One formate and one nitrate anion occupy the same coordination site on Pb1 and they have been given occupancy factors of 0.5 each; the corresponding nitrogen and carbon atoms were constrained to have the same position and displacement parameters. The solvent water molecule (O16) was given an occupancy factor of 0.5 so as to account for a close contact with its image by symmetry.

Crystal data and structure refinement parameters are given in Table 1. The molecular plots were drawn with ORTEP-3[55] and the polyhedral representations with VESTA.[56] The topological analyses were made with TOPOS.[57,58]

Luminescence Measurements. Emission spectra were recorded on solid samples using a Horiba-Jobin-Yvon Fluorolog spectrofluorometer. The powdered complex was pressed between two silica plates which were mounted such that the faces were oriented vertically and at 45° to the incident excitation radiation. An excitation wavelength of 420 nm was used in all cases and the emissions monitored between 450 and 650 nm.

RESULTS AND DISCUSSION

Synthesis. Complexes **1**–**10** were synthesized under either purely hydrothermal or solvo-hydrothermal conditions at 140 °C. In general, addition of an organic cosolvent is advantageous since it facilitates the initial formation of a homogeneous solution and prevents in some measure the formation of oligomeric uranyl species through hydrolysis, and also because it promotes the formation of novel species, either when it is retained as a neutral coligand, or through the ionic

coligands or the counterions generated by its own hydrolysis, probably catalyzed by the metal ions present (see below). Its effect on the solubility of the products may also influence the outcome of the crystallization process. In the present cases, the organic cosolvent was methanol for complex **1**, *N,N*-dimethylformamide (DMF) for **2**, **6** and **10**, acetonitrile for **4**, **5**, **8** and **9**, and *N*-methyl-2-pyrrolidone (NMP) for **7**. It is notable that organic cosolvents were only retained as intact coligands in the final compounds in the two cases of silver-bound acetonitrile in **4** and uranium-bound NMP in **7**. The crystals appeared during the heating phase and their presence in the glass vials was checked visually. To avoid hydrolytic oligomerisation of the uranyl cation, the carboxylate ligands were added in their acid form (generated in situ from the dianhydride in the case of H_4bptc) and in the absence of any base, the isolated solids nonetheless containing only the fully ionized acid anions. Systematic attempts with different organic cosolvents and with or without the additional presence of *N*-donors have been made with each acid and both Ag^{I} and Pb^{II}, the complexes reported here corresponding to the only cases in which crystals suitable for diffraction were obtained (in yields that are in most cases moderate or low). Formation of formate anions through DMF hydrolysis, resulting in fragmentary incorporation of the cosolvent as observed for complex **10**, is a common phenomenon.[16,59–63]

Crystal Structures. Both silver(I)- and lead(II)-containing compounds were obtained in the case of the long-chain (C_7) aliphatic pimelate ligand, $[Ag(bipy)_2]_2[UO_2(pim)(NO_3)]_2$ (**1**) and $[UO_2Pb(pim)_2(bipy)(H_2O)]\cdot 0.5bipy\cdot H_2O$ (**2**) (where bipy is 2,2′-bipyridine). Complex **1** has the same formula as a previously reported complex,[16] but a slightly different structure; the syntheses of these complexes differ in the stoichiometry of the reactants and the organic solvent used, acetonitrile in the previous case and methanol here. The asymmetric unit in **1** contains two

independent uranium atoms, pim^{2-} ligands and nitrate anions pertaining to two separate but identical units, two silver(I) ions and four bipy molecules (Figure 1). Each uranyl ion is chelated by two carboxylate groups from two ligands and one nitrate anion; the U–O(oxo) [1.763(3)–1.771(3) Å, average 1.767(3) Å], U–O(carboxylate) [2.425(4)–2.456(4) Å, average 2.439(10) Å] and U–O(nitrate) bond lengths [2.511(4)–2.530(3) Å, average 2.521(8) Å] are unexceptional. Each silver(I) ion is chelated by two bipy molecules, with Ag–N bond lengths of 2.286(4)–2.390(5) Å [average 2.34(4) Å], and the two $Ag(bipy)_2^+$ groups are associated through an argentophilic bonding interaction clearly evident in the Hirshfeld surface[64-66] generated with CrystalExplorer[67] (see Supporting Information), with an Ag1–Ag2 distance of 3.3071(6) Å shorter than twice the van der Waals radius of silver (1.72 Å). All four bipy units within a dimer are inequivalent, Ag–N distances within three of the chelate rings being markedly unsymmetrical [2.299(4), 2.370(5); 2.327(4), 2.340(5); 2.288(6), 2.382(5); and 2.286(4), 2.390(5) Å] and all four ligands being significantly twisted about the central bonds [N3–C19–C20–N4 14.5(7)°; N5–C29–C30–N6 22.0(6)°; N7–C39–C40–N8 11.9(8)°; N9–C49–C50–N10 26.0(7)°]. This twisting may be a reflection of C···C interactions beyond dispersion (C···C ~3.30 Å) indicated in the Hirshfeld surface, which result in links both within and between dimer units to give a chain running along the *b* axis, with successive units being related by inversion, in which the inter-dimer Ag···Ag distances are 5.6696(10) and 5.8362(10) Å. The bipy molecules in the dimer are close to the eclipsed geometry and π-stacking interactions are probably present [centroid···centroid distances 3.668(4)–4.271(4) Å, dihedral angles 2.3(3)–14.4(3)°]. The dimers in the chains are tilted with respect to one another (Figure 1) in such manner that inter-dimer π-stacking interactions may still be present [centroid···centroid distances 3.662(4) and 4.094(3) Å, dihedral angles 11.7(3) and 22.7(3)°]. The counter-ions and their arrangement were similar in the previously reported complex,

with however some slight differences, the most conspicuous being that in the angle between the Ag–Ag axis and the average N_4 plane around each cation, 148.8° in the former case, and 163.1/166.3° here; the inter-dimer Ag···Ag separation was larger in the other complex, at 6.1 Å. These differences, however small, may be related to the different geometries of the uranyl complex itself. The uranyl pimelate units in **1** form one-dimensional (1D) linear chains directed along the *a* axis, with the nitrate anions all located on the same side and the pimelate ligand in its nearly planar, fully extended conformation with all C–C–C–C torsion angles being anti and the O–C–C–C ones anti or syn. In contrast, notwithstanding the similar conformation of the ligand, the chains in the former complex were of a zigzag form, with nitrate ions alternately located on opposite sides, a difference that results from the rotation of the direction of one pimelate ligand by 60° within the uranyl equatorial plane. The packing in **1** displays bilayers of anionic uranyl complexes parallel to (0 0 1), separated from one another by the counter-ions, a feature that was absent in the previous case. The value of 0.69 found for the Kitaigorodski packing index (KPI, estimated with PLATON[54]) indicates that no free space is present (the usual values for non-porous packings being of the order of 0.65).

The lead(II)-containing complex **2** associates both metal cations within a single complex unit. The asymmetric unit contains one octacoordinate uranium cation chelated by three carboxylate groups from three pimelate ligands, and one lead(II) cation chelated by one carboxylate and one bipy ligand, and further bound to one carboxylate oxygen atom and one water molecule (Figure 2). The U–O(oxo) and U–O(carboxylate) bond lengths are in the usual ranges [1.762(3) and 1.763(3) Å, and 2.451(3)–2.488(3) Å (average 2.464(14) Å), respectively]. The Pb–O(chelating) bond lengths of 2.404(3) and 2.522(3) Å, and the Pb–N bond lengths of 2.461(4) and 2.513(3) Å are well within the usual ranges for similar motifs reported in the Cambridge Structural

Database (CSD, Version 5.37),[68] with large distributions centered at ~2.55 Å. The bond with the bridging atom O6 is longer, at 2.794(3) Å, and that with the water molecule even more so, at 2.919(4) Å; the latter is at the upper end of the range found in the CSD for Pb–O(water) bond lengths, 2.27–3.03 Å [average 2.63(15) Å]. A longer contact [Pb1···O3^{m} 3.091(3) Å, symmetry code: m = 1 – *x*, 1 – *y*, 2 – *z*] is also possibly associated to a bonding interaction, the limit chosen for the definition of true bonds being somewhat arbitrary,[28] although the calculation of Hirshfeld surfaces can be used to define interactions greater than dispersion, ideally with structures free of disorder, and indeed indicates clearly the presence of an interaction here. The environment of the hexacoordinate lead(II) ion appears to be hemidirected (even when the Pb1···O3^{m} contact is taken into account), an unsurprising result considering the somewhat low coordination number.[26] Two oxygen atoms, from carboxylate and uranyl groups, make much more distant approaches within the free region of space corresponding to the lead(II) lone pair [Pb1···O5^{i} 3.605(3) and Pb1···O2 3.795(3) Å, symmetry code: i = *x*, *y* – 1, *z*] but here, on the basis of the Hirshfeld surface, neither corresponds to an interaction greater than that of dispersion. The pimelate ligand containing atoms O3–O6 is in the nearly planar fully extended conformation, but that containing O7–O10 is buckled, with three C–C–C–C torsion angles being gauche instead of anti. So, while the former ligand, chelating one uranyl ion at each end, generates a linear 1D subunit directed along the *b* axis, two such strands are associated through the lead(II) cations and the curved ligand which connects the two different metal centres. The resulting assembly is a thick 1D polymer which could be seen as nanotubular in shape (albeit with an exceedingly small diameter) if it were not flattened. Adjacent chains in planes parallel to (0 0 1) are linked to one another by hydrogen bonds involving the coordinated and the lattice water molecules, and the centrosymmetric free bipy molecule [O···O/N 2.819(4)–3.111(7) Å, H···O/N 1.96–2.26 Å, O–H···O/N 144–163°]. A π-stacking interaction links

two aromatic rings of coordinated bipy molecules in different hydrogen bonded layers [centroid···centroid distance 3.777(2) Å, dihedral angle 9.8(2)°] and two CH(aliphatic)···π interactions may also be present [H···centroid distances 2.58 and 2.84 Å, C–H···centroid angles 148 and 138°], all these interactions resulting in a compact packing with a KPI of 0.71. Comparison of the structures of complexes **1** and **2** illustrates the different roles of the cations Ag^{I} and Pb^{II}. The affinity of the former for nitrogen donors and its propensity to form dimers through argentophilic interactions lead to its segregation in the form of a dissociated counter-ion, while the latter competes with uranium for the carboxylate donors and is as a result part of a neutral, heterometallic coordination polymer. Note that the free bipy molecule present in **2** has the anticipated transoid configuration as distinct from the cisoid conformation of the coordinated species,[69] the structure of **2** providing another example of the need of a crystal structure determination to establish whether or not a given ligand is coordinated with labile metal ion species.

Two silver-containing complexes were obtained with the $chtc^{3-}$ ligand, without or with coordinated bipy molecules, $[UO_2Ag(chtc)(H_2O)_2]$ (**3**) and $[Ag(bipy)(CH_3CN)]_2[UO_2(chtc)]_2$ (**4**), but no solid material was deposited from an experiment analogous to that giving complex **3**, in which Ag^{I} was replaced by Pb^{II}. The asymmetric unit in complex **3** contains one uranyl cation chelated by three carboxylate groups, with U–O(carboxylate) bond lengths of 2.433(4)–2.508(4) Å [average 2.47(3) Å], as usual for the hexagonal bipyramidal coordination environment, one silver(I) cation in a general position, and one $chtc^{3-}$ ligand in the chair conformation with all carboxylate groups equatorial (Figure 3). The silver centre is bound to one oxygen atom from a carboxylate group which chelates uranium, thus forming a μ_2-κ^1O:κ^2O,O' bridge between the two metal cations [Ag–O bond length 2.384(3) Å], two water molecules [2.263(6) and 2.379(5) Å] and the uranyl oxo atom O1 at 2.464(4) Å. The latter distance is indicative of genuine oxo bonding, the

bond lengths reported in the other known cases being in the range 2.38–2.58 Å.[20–22] The U–O1 bond length is however not significantly longer than U–O2 [1.790(4) versus 1.774(4) Å]. The coordination environment of Ag1 is a very distorted tetrahedron, with however a fifth, longer contact with atom $O7^{ii}$ at 2.875(4) Å (symmetry code: ii = 1 – *x*, *y* – 1/2, 2 – *z*). The uranyl ions and $chtc^{3-}$ ligands alone form a two-dimensional (2D) honeycomb network parallel to (1 0 –1), with the point (Schläfli) symbol $\{6^3\}$, analogous to those previously found in several uranyl complexes with this ligand.[46] When viewed perpendicular to these layers, the silver(I) cations seem like appendages located in the hexagonal cells while, when viewed with layers edge-on, the silver–oxo bonds are seen to connect adjacent sheets, thus forming a 3D framework. If the silver atoms are considered as simple links, the point symbol of the whole network is $\{6^6\}$ and it corresponds to the lon topological type, called thus in reference to lonsdaleite or hexagonal diamond.[70] The coordinated water molecules are hydrogen bonded to one another and to carboxylate oxygen atoms [O···O 2.680(5)–3.127(7) Å, H···O 1.81–2.33 Å, O–H···O 136–173°], and the packing does not display any solvent-accessible space (KPI 0.73).

The addition of bipy in complex **4** has the effect of separating the counter-ion in the form of the dimer $\{[Ag(bipy)(CH_3CN)]_2\}^{2+}$. As in complex **3**, the single uranyl ion is chelated by three carboxylate groups with U–O(carboxylate) bond lengths of 2.434(11)–2.488(11) Å [average 2.46(2) Å] and, together with the $chtc^{3-}$ ligand in the chair conformation, it forms the usual honeycomb network (Figure 4). The unique Ag^I cation is chelated by the bipy molecule [Ag–N bond lengths of 2.258(15) and 2.321(16) Å] and bound to an acetonitrile molecule [2.098(17) Å] as well as being involved in an argentophilic interaction with its image by inversion [3.257(3) Å]. The three *N*-donors are in a plane containing the Ag^I cation, and the coordination environment is thus trigonal pyramidal. However, the existence of a longer contact, at 2.938(12) Å, with the uranyl

oxo atom $O1^{ii}$ (symmetry code: ii = 3/2 – *x*, *y* – 1/2, 1/2 – *z*) indicates that the bridging of layers found in **3** is not completely obliterated, but the oxo bonding is weak at best (as confirmed by the difference between the two U–O(oxo) bond lengths, 1.789(11) and 1.778(11) Å for O1 and O2, respectively, which is not significant), even though clearly apparent on the Hirshfeld surface. As with Pb(II), it is not uncommon to find for Ag(I) that a precise definition of its coordination sphere is difficult to obtain. A possible parallel-displaced π-stacking interaction links adjacent silver dimers within the inter-sheet space [centroid···centroid distance 4.125(10) Å, dihedral angle 0°]. Here also, no solvent-accessible space is present (KPI 0.70).

Two heterometallic complexes were obtained with the $bptc^{4-}$ ligand, $[UO_2Ag(bptc)(4,4'\text{-bipyH})]$ (**5**) and $[UO_2Pb(bptc)(bipy)_2]$ (**6**), this being a second case in which it was possible to obtain crystals of compounds with both Ag^I and Pb^{II} cations. The asymmetric unit in **5** contains one uranyl cation chelated by one carboxylate group and bound to three more carboxylate oxygen atoms from three different ligands, the uranium coordination environment being thus pentagonal bipyramidal (Figure 5). The U–O(oxo) bond lengths of 1.776(2) Å, and the U–O(carboxylate) bond lengths of 2.468(2) and 2.478(2) Å for the chelating group, and 2.299(2)–2.346(2) Å for the three other carboxylate donors are unexceptional. The unique silver(I) cation is bound to two carboxylate groups from two ligands [Ag–O bond lengths of 2.158(2) and 2.524(2) Å, the former being in the lower part of the range for Ag–O(carboxylate) bond lengths found from the CSD, which are widely distributed between ~2.1 and 2.9 Å]; it is also bound to one nitrogen atom from 4,4′-bipyridine, at 2.175(3) Å [average 2.18(6) Å from the CSD]. A longer contact with atom O4 at 2.713(2) Å completes the very irregular four-coordinate silver environment. One source of this irregularity may be the proximity of the pyridyl ring *N*-bound to an adjacent Ag^I centre. The centroid of this pyridyl ring is at 3.39 Å from Ag^I, with a near-symmetric positioning resulting in Ag···C distances

ranging from 3.611(4) to 3.689(4) Å and Ag···N 3.666(3) Å. Although possibly an indication of a hexahapto aromatic interaction, of which examples may also be found in Pb^{II} chemistry,[71] the Hirshfeld surface for the asymmetric unit of **5** provides no evidence of interactions beyond dispersion. The two aromatic rings of the $bptc^{4-}$ ligand are close to coplanarity, with a dihedral angle of 9.67(5)°, but, as might be expected given their proximity, adjacent carboxylate groups are not coplanar and the four carboxylate groups are rotated with respect to the aromatic ring to which they are attached, the dihedral angles being 20.99(19), 75.98(12), 72.68(13) and 18.22(11)°, the groups containing the pairs of atoms O5, O6 and O7, O8 being the more tilted. This ligand is bound to six (four U^{VI} and two Ag^{I}) metal atoms, with κ^1O, μ_2-κ^1O:κ^1O', and μ_2-κ^1O:κ^2O,O' carboxylate coordination modes. The resulting coordination polymer, despite the twisting of the donor groups into planes inclined at more than 50°, has only a buckled 2D form parallel to (0 0 1), and it is notable that Ag^{I} plays no topological role, being a simple appendage to the layers, the four-fold uranium and $bptc^{4-}$ nodes defining the common $\{4^4.6^2\}$ Shubnikov tetragonal plane net (sql) topology. The 4,4′-bipyH^+ cation, protonated at one end, lies in a stacked array nearly parallel to a $bptc^{4-}$ ligand in the same layer and to another in the neighbouring layer along the *c* axis, with possible π-stacking interactions [centroid···centroid distances 3.5983(16)–3.7469(18) Å, dihedral angles 2.47(13)–12.02(15)°]; it is also involved in a hydrogen bond between the protonated nitrogen atom and an uncoordinated carboxylate oxygen atom of the same layer [N2···$O6^m$ 2.708(3) Å, H···$O6^m$ 1.76 Å, N2–H···$O6^m$ 170°; symmetry code: m = 1 – *x*, *y* – 1/2, 3/2 – *z*], and in a CH···O interaction apparent on the Hirshfeld surface. The similar length of these two ligands, and their parallel location on the two sides of the sheets result in the latter having a bilayer appearance when viewed down the *a* axis (Figure 5). No significant free space is present either within or between the layers, and the KPI value is 0.72.

The asymmetric unit in complex **6** contains one uranium atom located on an inversion centre, which is chelated by two carboxylate groups and bound to two more carboxylate oxygen atoms, the coordination environment being thus hexagonal bipyramidal (Figure 6). The U–O(oxo) bond length of 1.771(3) Å, and the U–O(carboxylate) bond lengths of 2.507(3) and 2.525(3) Å for the chelating group, and 2.390(3) Å for the monodentate ones are unexceptional. The octa-coordinate lead(II) cation, located on a twofold rotation axis, is chelated by two bipy molecules and by two carboxylate groups, with Pb–N bond lengths of 2.601(4) and 2.676(4) Å, and Pb–O bond lengths of 2.770(3) and 2.870(3) Å. These distances are longer than in complex **2**, probably due to the higher coordination number, and two even longer contacts, with O4 and its image by symmetry, at 3.269(4) Å, exceed the usual limit for bonding interactions with lead(II), although the Hirshfeld surface indicates that these interactions exceed dispersion forces. The geometry of the Pb^{II} coordination sphere is very irregular but with no obvious hemi- or holodirected proclivity. The two aromatic rings of the ligand, related by a twofold rotation axis, are more tilted with respect to one another than in complex **5**, the dihedral angle being 65.41(15)°, and the two carboxylate groups on each ring are here also rotated differently, with dihedral angles of 72.6(3) and 9.4(8)° for the groups containing the pairs O2, O3 and O4, O5, respectively. Each $bptc^{4-}$ ligand connects six metal cations (four uranyl and two lead(II) cations) with κ^2O,O' and μ_2-κ^1O:κ^2O,O' coordination modes. The uranium atoms and $bptc^{4-}$ ligands are four-fold nodes and the 2D assembly formed, parallel to (0 1 0), has the same $\{4^4.6^2\}$ topology as that in **5**, notwithstanding the differences in ligand geometry and carboxylate bonding mode, although the ligand units in a given 2D assembly are close to a common mean plane, unlike the stepped arrangement found in **5**. As well, while the Ag(4,4′-bipyH)$^{2+}$ groups in **5** are arranged parallel to the layers, the Pb(bipy)$_2^{2+}$ groups here are protruding appendages on the two sides of the layers, adjacent sheets along the *b*

axis being interlocked, with bipy units of adjacent Pb^{II} centres forming stacked arrays [centroid···centroid distances 3.855(3) and 4.364(3) Å, dihedral angles 0 and 12.9(3)°], although the Hirshfeld surface indicates that the principal interactions beyond dispersion linking layers are of CH(bipy)···O($bptc^{4-}$) (H···O distances 2.35–2.52 Å,) and CH($bptc^{4-}$)···C(bipy) (H···C distance 2.79 Å) types. A weak CH(bipy)···π hydrogen bond [H···centroid distance 2.97 Å, C–H···centroid angle 119°] may also be present. The packing has a KPI of 0.73 and is thus quite compact.

The difference in the nature of the *N*-donor in complexes **5** and **6** means that the two compounds are not exactly comparable. However, in spite of this difference, there are some common points: in both complexes, the $bptc^{4-}$ ligand is bound to both uranyl and the additional cation, and 2D uranyl–$bptc^{4-}$ anionic subunits of identical topologies are formed, the additional metal ions and *N*-donors being incorporated as mere decorating species. The presence of the bipyridine molecules, particularly in **6** where they occupy half the space around Pb^{II}, results in no dimensionality increase being brought about by the silver(I) or lead(II) cations. It may be noted that, probably due to the presence of the basic bipyridine molecules, H_4bptc is fully deprotonated here (and 4,4′-bipy is half-protonated as a result in **5**), whereas, in the complex obtained from H_4bptc (generated from the dianhydride) and uranyl ions alone, two carboxylate groups retain their proton and are uncoordinated, the dimensionality being reduced in this case to one.[47] As an aside, and although complex **7**, $[(UO_2)_2(bptc)(NMP)_{1.5}(H_2O)_{1.5}]\cdot 1.5H_2O$, does not properly belong to the present series, it is worth mentioning it here since, as observed with several other polycarboxylic acids,[46,72] the presence of coordinated NMP molecules results in the formation of a 3D framework, an outcome which could not be attained through the use of additional metal cations with this ligand. Of the two independent uranyl ions in the asymmetric unit of **7**, one (U1) is chelated by one carboxylate group and bound to one monodentate carboxylate oxygen atom and two NMP

molecules (one of them disordered, see Experimental), and the other (U2) is chelated by two carboxylate groups and bound to one monodentate carboxylate and one water molecule (Figure 7). There is nothing unusual in the U–O(oxo) [1.759(6)–1.769(7) Å], U–O(chelating carboxylate) [2.462(6)–2.558(6) Å], U–O(monodentate carboxylate) [2.308(5) and 2.431(6) Å], and U–O(NMP) [2.313(8) and 2.353(7) Å] bond lengths (the latter being in the range 2.33–2.44 Å in the structures previously reported[46]). The $bptc^{4-}$ anion is bound to five metal cations, with the κ^2O,O' (three times) and μ_2-κ^1O:κ^1O' (once) carboxylate coordination modes; its two aromatic rings make a dihedral angle of 19.4(4)°, and the four carboxylate groups are tilted by 71.3(5), 9.6(5), 67.5(6) and 20.9(5)° (in the order of increasing atom numbering) with respect to the attached aromatic ring. The 3D framework formed has the point symbol $\{6^3\}\{6^5.8\}$ and the topological type InS 3,4-conn of the topos&RCSR database. When viewed down the *b* axis, the framework displays layers built from U2 and the tetracarboxylate ligand parallel to (0 0 1), which are connected one to the other by U1 and its symmetry equivalents, while, when viewed down the *a* axis, channels occupied by the NMP molecules are apparent, the KPI being 0.72 (if the disorder affecting one NMP molecule is disregarded). The coordinated water molecule is hydrogen bonded to a uranyl oxo group and to a free water molecule [O···O distances 2.780(9) and 2.658(14) Å, H···O 2.06 and 1.89 Å, O–H···O angles 128 and 138°]. No π-stacking interaction is present, but one of the aromatic rings is involved in two CH···π hydrogen bonds with NMP methyl groups [H···centroid distances 2.82 and 2.96 Å, C–H···centroid angle 149° for both]. 3D frameworks displaying channels containing coordinated NMP molecules have previously been found with polycarboxylic acids as diverse as terephthalic, 2,5-thiophenedicarboxylic, nitrilotriacetic,[72] and 1,3,5-cyclohexanetricarboxylic[46] acids, a characteristic of all these compounds and thus a drawback with respect to possible applications, being their lack of porosity.

Only one complex of 3-pyrimidin-2-yl-benzoic acid with the uranyl cation (or in fact any metal cation) has previously been reported, $[Ni(phen)_3][UO_2(pyb)_3]_2 \cdot 2.5H_2O$, in which the uranyl cation is chelated by three carboxylate groups, and the pyrimidyl nitrogen atoms are uncoordinated.[48] These nitrogen donors are well suited for complexation of a metal cation such as Ag^I, as confirmed by the structure of the heterometallic complex $[UO_2Ag(pyb)_3(H_2O)_2] \cdot 4H_2O$ (**8**). In this complex again, the unique uranium atom is chelated by the carboxylate groups of three pyb^- ligands, with U–O bond lengths of 2.448(4)–2.501(4) Å (Figure 8). As in the previous complex, instead of being arranged in a triskelion-like shape around the metal cation, two of the pyrimidinyl units are facing each other so as to form a cleft or tweezer, different however from the usual aromatic clefts in that the two rings are nearly coplanar. The silver atom is bound to two nitrogen atoms from two pyb^- ligands, one of them (N3) being from the cleft, the latter being however too large for silver(I) to be bound to both N3 and N5, which are 8.471(8) Å apart. The Ag–N bond lengths are 2.443(5) and 2.273(5) Å for N1 and N3, respectively. Two water molecules are also coordinated, with Ag–O bond lengths of 2.430(5) and 2.327(6) Å for O9 and O10, respectively, and a longer contact with the uranyl oxo atom O1 at 3.005(4) Å is possibly indicative of uranyl oxo bonding, although the Ag–O distance is much larger than that in complex **3** and other cases of clearcut oxo bonding.[20–22] The weakness of the latter interaction is also shown by the absence of significant lengthening of the corresponding U–O bond length [1.782(4) Å versus 1.773(4) Å for O2]. That the interaction nonetheless exceeds dispersion is indicated by the Hirshfeld surface, which also provides evidence for an Ag···H interaction [2.49 Å]. Thus, the coordination environment of Ag^I is difficult to describe, being highly distorted octahedral if the Ag···H interaction is included, slightly distorted trigonal bipyramidal, with atoms N1 and $O1^j$ in axial positions [N1–Ag1–$O1^j$ angle 160.47(15)°] if it is not, or trigonal pyramidal if oxo bonding is also

disregarded. Two of the ligands bound to uranium are connected to silver cations through one of their nitrogen atoms, while the third is terminal. The ensuing 1D polymer, parallel to the *a* axis, is dimerized into a double chain, with the terminal ligands protruding on two sides, if the oxo bonds are taken into account. All three ligands on a given uranyl centre can be regarded as sandwiched within stacked arrays involving ligands from other centres and five short contacts between aromatic rings may be indicative of parallel-displaced π-stacking interactions, both intra- and inter-chain [centroid···centroid distances 3.691(4)–3.988(4) Å, dihedral angles 0.9(4)–14.0(3)°], although examination of the Hirshfeld surface provides little evidence that they exceed dispersion, their importance being at most moderate. The most prominent interactions in the packing are OH···O hydrogen bonds, with the coordinated and free water molecules bound to one another and to carboxylate oxygen atoms, with also a bond involving atom N5, a lattice water molecule making a link between the coordinated water molecule containing O10 and this uncoordinated atom of the cleft. Although not all water hydrogen atoms have been found, those present give rise to the formation of sheets parallel to (0 0 1), the packing being quite compact, with a KPI of 0.73.

Attempts to synthesize a heterometallic complex of Hpyb with uranyl and lead(II) cations failed to give any exploitable material, and only in one case (with additional bipy molecules) was it possible to isolate a molecular, homometallic uranyl complex, $[UO_2(pyb)_2(bipy)]$ (**9**), which will be briefly described for comparison with complex **8**. The unique uranium atom is chelated by two carboxylate groups, the two pyb^- ligands being arranged in cleft-like fashion, and by a bipy molecule (Figure 9). The U–O(oxo) [1.753(6) and 1.776(6) Å], U–O(carboxylate) [2.440(6)–2.481(6) Å] and U–N [2.606(6) and 2.711(7) Å] bond lengths are unremarkable, as is also the departure from planarity of the uranyl equatorial set of donor atoms, with the bipy molecule making a dihedral angle of 36.33(15)° with the average plane defined by U1 and the four carboxylate

donors, a value well within the usual range.[35] Four short contacts between aromatic rings pertaining to both bipy and pyb^- ligands are indicative of parallel-displaced π-stacking interactions [centroid···centroid distances 3.598(5)–4.062(5) Å, dihedral angles 0.7(4)–17.3(4)°], that appear to be of moderate strength from Hirshfeld surface analysis. In this case where water molecules are absent and the complex is neutral, weak CH···O hydrogen bonds[73–75] may play a significant role, and several are apparent. In particular, one bipy aromatic ring is located in the cleft of a neighbouring molecule, and forms two such bonds with the carboxylate atoms O4 and O5 [H···O distances 2.706 and 2.715 Å, respectively]. With a KPI of 0.72, the packing contains no solvent-accessible space.

2,6-Pyridinedicarboxylic acid has been very often used in uranyl chemistry,[11,36–45] and the complex $[UO_2Pb_2(pydc)_2(phen)_2(HCOO)_{1.5}(NO_3)_{0.5}]\cdot 0.5H_2O$ (**10**) is the third case of a uranyl–lead(II) heterometallic complex, after $[UO_2Pb_2(pydc)_2(C_2O_4)(H_2O)_2]$, that also contains oxalate ligands, and $[UO_2Pb(pydc)_2]\cdot 2H_2O$, that both crystallize as 3D assemblies.[11] This former report described also a uranyl–silver(I) heterometallic complex, but no such species including bipy or phen ligands could be crystallized for comparison with complex **10**. The asymmetric unit in **10** contains one uranyl cation bound to the *O,N,O* site of two $pydc^{2-}$ ligands, as usual, with U–O(carboxylate) bond lengths of 2.429(2)–2.451(3) Å and U–N bond lengths of 2.652(3) and 2.659(3) Å. As in the previously reported complex, one lead(II) cation is attached on each side of this unit through the four bridging carboxylate atoms, one carboxylate group in each case being chelating in a very asymmetric way (Figure 10). Each Pb^{II} cation is also chelated by a phen molecule and a formate anion formed in situ from DMF hydrolysis, with formate/nitrate disorder in one case (see Experimental); in contrast to the bridging oxalate co-ligands found in the previously reported structure, the formate anions are terminal. Both Pb1 and Pb2 are further

involved in a weaker bond to one carboxylate donor from another unit, (in the case of Pb1, this results in O3 being bound to three metal ions). Moreover, Pb1 is probably involved in a bonding interaction with the oxo atom $O1^{i}$ at 3.007(2) Å. The latter distance is close to that of 2.999(4) Å found in another uranyl–lead(II) heterometallic complex,[18] and the significant lengthening of the corresponding U–O1 bond length [1.777(2) Å versus 1.754(2) Å for O2] confirms the presence of a bonding interaction. The Pb–N [2.587(3)–2.657(3) Å] and Pb–O(carboxylate) [2.498(2)–3.069(2) Å] bond lengths span the usual large ranges. The coordination numbers are 9 and 8 for Pb1 and Pb2, respectively, the environments being in both cases very irregular but essentially holodirected. In the simple Pb^{II} complex of pydc, $[Pb(pydc)(H_2pydc)(H_2O)_3]$,[76] the metal ion is 9-coordinate in a hemidirected array, proposed to be a consequence of stacking interactions rather than of a lone pair effect. Bridging of the $UO_2(pydc)_2^{2-}$ units by groups of two lead(II) centres leads to the formation of a 1D polymer directed along the [1 1 1] axis. The presence of parallel-displaced π-stacking interactions, both intra- and inter-chain, is suggested by six centroid···centroid distances in the range 3.646(2)–4.126(2) Å [dihedral angles 4.22(18)–30.11(18)°]; here also, both intra- and inter-chain CH···O bonding may be present, with H···O distances as short as 2.46 Å, the most conspicuous being those between the uncoordinated or loosely coordinated carboxylate atoms O4, O6, O8 and O10 and hydrogen atoms of the phen molecules. With a KPI of 0.74, the packing is a very compact one. As previously noticed for several heterometallic complexes with this ligand,[11] binding of uranyl and lead(II) centres in this complex does not match what could be expected from HSAB considerations, the harder uranium metal ion being bound to the softer nitrogen donor. Uranyl coordination by the tridentate *O,N,O* site from one or two ligands, forming two five-membered chelate rings, is pervasive in both homo- and heterometallic species with $pydc^{2-}$, this

particularly strong affinity of uranyl resulting in the relegation of any other metal cation at the periphery of the uranyl complex motif.

Luminescence Properties. Emission spectra were recorded at room temperature for all complexes but **6** (for which a sufficient amount of pure crystals could not be isolated), in the solid state and under excitation at a wavelength of 420 nm, a value suitable for uranyl excitation and corresponding to the U=O axial LMCT band,[77,78] and they are shown in Figure 11. Nearly complete quenching of uranyl luminescence occurs for complexes **3**, **8** and **10**, the two former containing silver(I) and the last lead(II) cations. Although it is not general, as witnessed by several of the complexes reported here, quenching has previously been observed in uranyl–silver(I) heterometallic complexes,[14,17,18] and it has been assigned to the silver(I) cations providing a nonradiative relaxation pathway;[14] quenching has also been reported in a uranyl–lead(II) complex, but here also this is not a general phenomenon.[18] The weak luminescence in the solid state observed for **10** contrasts with what appear to be cases of aggregation-enhanced emission observed in the alkali metal ion derivatives of $[UO_2(pydc)_2]^{2-}$,[39] and may reflect the absence of extended stacking of the pydc entities in the lattice of **10**. For all the other complexes in the present series, the vibronic progression corresponding to the $S_{11} \rightarrow S_{00}$ and $S_{10} \rightarrow S_{0\nu}$ ($\nu = 0$–4) electronic transitions that is usual for uranyl compounds[79] is apparent, with four or five well-resolved peaks displaying well-marked variations in the maxima positions. In the case of the homometallic complex **9**, these positions (471, 486, 506, 528 and 552 nm) are close to those measured in other complexes with eight-coordinate uranium cations including two carboxylate and one chelating *N*-donor as ligands,[35] while those for the eight-coordinate complexes **1** (481, 501, 523 and 547 nm) and **2** (482, 502, 524 and ~545 nm) are displaced toward short wavelengths by 5 or 4 nm, respectively (the

first, weak peak observed in **9** being unobservable here), and are close to those previously measured in several eight-coordinate uranyl carboxylate complexes.[7,16,17,34,35,46,63,72,80] The positions for complex **4** are slightly more red-shifted (489, 509, 531 and 555 nm), although carboxylate ter-chelation is present here also. Finally, the maxima positions for complexes **5** (496, 516, 539 and 564 nm) and **7** (493, 514, 538 and 563 nm) are the most red-shifted in this series and it is probably no accident that these complexes contain either purely seven-coordinate uranium cations (**5**) or a mixture of eight- and seven-coordinate ones (**6**). Such red-shift of the spectra for uranyl species with five equatorial donors has previously been noticed,[7,8,63,72,81–83] although it is by no means general since the coordination number is only one factor at play, variations in the strength of the ligands having also an effect.[84,85]

CONCLUSIONS

The five mono- or polycarboxylate ligands used to synthesize the present series of eight heterometallic complexes containing uranyl and either silver(I) or lead(II) cations, have provided a useful basis to the study of the effects of the latter additional cations, whether included as simple counter-ions or integrated in a mixed-metal coordination polymer, on the geometry and dimensionality of the species formed. Additional cations are often added during the synthesis of uranyl–organic coordination polymers so as to introduce multi-directional linkers in systems that, due to the linear shape of the uranyl cation and its peculiar planar coordination preferences, are particularly prone to give 1D or 2D quasi-planar architectures. This expectation has been met here in the uranyl–silver(I) complex with $chtc^{3-}$ (**3**), in which 2D uranyl carboxylate subunits analogous to those generally obtained with this ligand are assembled into a 3D framework through carboxylate- and oxo-bound Ag^{I} cations. Further addition of bipy molecules results in the separation of the latter cations to form $[Ag(bipy)(CH_3CN)]^{+}$ counter-ions, dimerized through

argentophilic interactions, as found in complex **4**, which retains a 2D structure. Even when such an increase in dimensionality as that found in **3** is absent, the presence of Ag^{I} or Pb^{II} may bring about novel connectivities. Unsurprisingly, these two cations behave differently in complexes **1** and **2** involving the pimelate ligand and bipy molecules; while Ag^{I} forms separate $\{[Ag(bipy)_2]_2\}^{2+}$ counter-ions, the higher affinity of Pb^{II} for carboxylates and its capacity to adopt high coordination numbers are the cause of its being part of a heterometallic 1D polymer. This is however not always so, and, in spite of different *N*-donors being used, complexes **5** and **6**, with $bptc^{4-}$, display uranyl polycarboxylate 2D subunits of identical topology, the additional cations being in both cases mere carboxylate-bound appendages. It is notable that the ligand pyb^{-}, which possesses two nitrogen donors in its pyrimidinyl group, gives a heterometallic 1D species (**8**) in which, as expected, Ag^{I} is bound to nitrogen atoms but not to carboxylate groups, while no heterometallic complex could be crystallized with Pb^{II}. Complex **8** is an illustration of what can be expected from HSAB considerations, but, as previously noted, this simple picture is often disturbed by other features such as the affinity of uranyl for the *O,N,O* site of $pydc^{2-}$,[11] as shown by complex **10**. An interesting feature of the present structures, one which reflects their broader context, concerns the coordination spheres of Ag^{I} and Pb^{II}. In most instances, the metal ions can be said to have markedly irregular coordination spheres, with up to three donor atoms at distances up to 0.5 Å longer than those considered to be closest and thus presumably involved in weaker interactions. While in the case of Pb^{II} this is a situation conventionally attributed to the effects of a valence shell lone pair, this cannot be the case for Ag^{I}, where the filled 4d shell should be spherically symmetrical. An explanation may be that the relatively weak coordinative interactions of these two metal ions involve energies comparable to those of ligand-ligand repulsions and interspecies interactions in the solid state, meaning of course that the unusual coordination geometry should be taken as a characteristic of the crystalline lattice and not necessarily of species formed on dissolution in a solvent. Apart from

three cases in which uranyl luminescence is completely quenched, the emission spectrum of most other complexes in this series displays the usual vibronic fine structure with a rather close relation between the position of the maxima and the uranium coordination number (which is not necessarily valid more generally). A motivation for extending our previous studies was the possibility of obtaining porous frameworks, in particular those where the photochemical activity of the uranyl centres might be exploited, with possible control by the additional metal ions, but the fact that none of the lattices shows significant porosity prevents any practical use of the present compounds.

ASSOCIATED CONTENT

Supporting Information

The Supporting Information is available free of charge on the ACS Publications website at DOI:.

Hirshfeld surface analysis of complexes **1** and **8**, and views of Hirshfeld surfaces for all complexes (PDF)

Accession Codes

CCDC 1523098−1523107 contains the supplementary crystallographic data for this paper. These data can be obtained free of charge via www.ccdc.cam.ac.uk/data_request/cif, or by emailing data_request@ccdc.cam.ac.uk, or by contacting The Cambridge Crystallographic Data Centre, 12, Union Road, Cambridge CB2 1EZ, UK; fax: +44 1223 336033.

AUTHOR INFORMATION

Corresponding Authors

*E-mail: pierre.thuery@cea.fr (P. T.)

*E-mail: harrowfield@unistra.fr (J. H.)

Notes

The authors declare no competing financial interest.

REFERENCES

1 Cahill, C. L.; de Lill, D. T.; Frisch, M. *CrystEngComm* **2007**, *9*, 15–26.

2 Andrews, M. B.; Cahill, C. L. *Chem. Rev.* **2013**, *113*, 1121–1136.

3 Su, J.; Chen, J. S. *Struct. Bond.* **2015**, *163*, 265–296.

4 Wang, K. X.; Chen, J. S. *Acc. Chem. Res*. **2011**, *44*, 531–540.

5 Loiseau, T.; Mihalcea, I.; Henry, N.; Volkringer, C. *Coord. Chem. Rev.* **2014**, *266–267*, 69–109.

6 Thuéry, P. *Cryst. Growth Des.* **2014**, *14*, 901–904.

7 Thuéry, P.; Rivière, E.; Harrowfield, J. *Inorg. Chem.* **2015**, *54*, 2838–2850.

8 Thuéry, P.; Harrowfield, J. *Inorg. Chem.* **2015**, *54*, 8093–8102.

9 Thuéry, P. *Cryst. Growth Des.* **2016**, *16*, 546–549.

10 Yu, Z. T.; Liao, Z. L.; Jiang, Y. S.; Li, G. H.; Chen, J. S. *Chem.–Eur. J.* **2005**, *11*, 2642–2650.

11 Frisch, M.; Cahill, C. L. *Dalton Trans*. **2006**, 4679–4690.

12 Luo, G. G.; Lin, L. R.; Huang, R. B.; Zheng, L. S. *Dalton Trans*. **2007**, 3868–3870.

13 Liao, Z. L.; Li, G. D.; Bi, M. H.; Chen, J. S. *Inorg. Chem*. **2008**, *47*, 4844–4853.

14 Kerr, A. T.; Cahill, C. L. *Cryst. Growth Des*. **2014**, *14*, 1914–1921.

15 Thuéry, P.; Harrowfield, J. *CrystEngComm* **2016**, *18*, 1550–1562.

16 Thuéry, P.; Rivière, E.; Harrowfield, J. *Cryst. Growth Des*. **2016**, *16*, 2826–2835.

17 Thuéry, P.; Harrowfield, J. *Inorg. Chem.* **2016**, *55*, 6799–6816.

18 Thuéry, P.; Harrowfield, J. *Cryst. Growth Des*. **2016**, *16*, 7083–7093.

19 Yu, Y.; Zhan, W.; Albrecht-Schmitt, T. E. *Inorg. Chem*. **2007**, *46*, 10214–10220.

20 Adelani, P. O.; Albrecht-Schmitt, T. E. *Angew. Chem. Int. Ed.* **2010**, *49*, 8909–8911.

21 Adelani, P. O.; Albrecht-Schmitt, T. E. *Cryst. Growth Des.* **2012**, *12*, 5800–5805.

22 Nelson, A. G. D.; Rak, Z.; Albrecht-Schmitt, T. E.; Becker, U.; Ewing, R. C. *Inorg. Chem.* **2014**, *53*, 2787–2796.

23 Eckhardt, S.; Brunetto, P. S.; Gagnon, J.; Priebe, M.; Giese, B.; Fromm, K. M. *Chem. Rev.* **2013**, *113*, 4708–4754.

24 Schmidbaur, H.; Schier, A. *Angew. Chem. Int. Ed*. **2015**, *54*, 746–784.

25 Serezhkina, L. B.; Vologzhanina, A. V.; Klepov, V. V.; Serezhkin, V. N. *Crystallogr. Rep*. **2011**, *56*, 132–135.

26 Shimoni-Livny, L.; Glusker, J. P.; Bock, C. W. *Inorg. Chem.* **1998**, *37*, 1853–1867.

27 Hancock, R. D.; Reibenspies, J. H.; Maumela, H. *Inorg. Chem.* **2004**, *43*, 2981–2987.

28 Harrowfield, J. *Helv. Chim. Acta* **2005**, *88*, 2430–2432.

29 Hu, M. L.; Morsali, A.; Aboutorabi, L. *Coord. Chem. Rev.* **2011**, *255*, 2821–2859.

30 Romero, M. J.; Carballido, R.; Rodríguez-Silva, L.; Maneiro, M.; Zaragoza, G.; González-Noya, A. M.; Pedrido, R. *Dalton Trans.* **2016**, *45*, 16162–16165.

31 Borkowski, L. A.; Cahill, C. L. *Cryst. Growth Des*. **2006**, *6*, 2241–2247.

32 Borkowski, L. A.; Cahill, C. L. *Cryst. Growth Des*. **2006**, *6*, 2248–2259.

33 Thuéry, P. *Cryst. Growth Des*. **2011**, *11*, 2606–2620.

34 Thuéry, P.; Harrowfield, J. *Inorg. Chem.* **2016**, *55*, 2133–2145.

35 Thuéry, P.; Harrowfield, J. *CrystEngComm* **2016**, *18*, 3905–3918.

36 Marangoni, G.; Degetto, S.; Graziani, R.; Bombieri, G.; Forsellini, E. *J. Inorg. Nucl. Chem.* **1974**, *36*, 1787–1794.

37 Immirzi, A.; Bombieri, G.; Degetto, S.; Marangoni, G. *Acta Crystallogr., Sect. B* **1975**, *31*, 1023–1028.

38 Masci, B.; Thuéry, P. *Polyhedron* **2005**, *24*, 229–237.

39 Harrowfield, J. M.; Lugan, N.; Shahverdizadeh, G. H.; Soudi, A. A.; Thuéry, P. *Eur. J. Inorg. Chem.* **2006**, 389–396.

40 Jiang, Y. S.; Li, G. H.; Tian, Y.; Liao, Z. L.; Chen, J. S. *Inorg. Chem. Commun.* **2006**, *9*, 595–598.

41 Mirzaei, M.; Eshtiagh-Hosseini, H.; Lippolis, V.; Aghabozorg, H.; Kordestani, D.; Shokrollahi, A.; Aghaei, R.; Blake, A. J. *Inorg. Chim. Acta* **2011**, *370*, 141–149.

42 Xu, C.; Tian, G.; Teat, S. J.; Rao, L. *Inorg. Chem.* **2013**, *52*, 2750–2756.

43 Thuéry, P. *CrystEngComm* **2013**, *15*, 6533–6545.

44 Jayasinghe, A. S.; Unruh, D. K.; Kral, A.; Libo, A.; Forbes, T. Z. *Cryst. Growth Des*. **2015**, *15*, 4062–4070.

45 Qiu, J.; Vlaisavljevich, B.; Jouffret, L.; Nguyen, K.; Szymanowski, J. E. S.; Gagliardi, L.; Burns, P. C. *Inorg. Chem.* **2015**, *54*, 4445–4455.

46 Thuéry, P.; Harrowfield, J. *Cryst. Growth Des*. **2014**, *14*, 4214–4225.

47 Thuéry, P.; Masci, B. *CrystEngComm* **2012**, *14*, 131–137.

48 Thuéry, P. *Inorg. Chem. Commun.* **2015**, *59*, 25–27.

49 Hooft, R. W. W. *COLLECT*, Nonius BV: Delft, The Netherlands, 1998.

50 Otwinowski, Z.; Minor, W. *Methods Enzymol.* **1997**, *276*, 307–326.

51 Sheldrick, G. M. *Acta Crystallogr., Sect. A* **2015**, *71*, 3–8.

52 Sheldrick, G. M. *Acta Crystallogr., Sect. C* **2015**, *71*, 3–8.

53 Parsons, S.; Flack, H. D.; Wagner, T. *Acta Crystallogr., Sect. B* **2013**, *69*, 249–259.

54 Spek, A. L. *Acta Crystallogr., Sect. D* **2009**, *65*, 148–155.

55 Farrugia, L. J. *J. Appl. Crystallogr.* **2012**, *45,* 849–854.

56 Momma, K.; Izumi, F. *J. Appl. Crystallogr.* **2008**, *41,* 653–658.

57 Blatov, V. A.; Shevchenko, A. P.; Serezhkin V. N. *J. Appl. Crystallogr*. **2000**, *33*, 1193.

58 Blatov, V. A.; O'Keeffe, M.; Proserpio, D. M. *CrystEngComm* **2010**, *12*, 44–48.

59 Bilyk, A.; Dunlop, J. W.; Fuller, R. O.; Hall, A. K.; Harrowfield, J. M.; Hosseini, M. W.; Koutsantonis, G. A.; Murray, I. W.; Skelton, B. W.; Stamps, R. L.; White, A. H. *Eur. J. Inorg. Chem.* **2010**, 2106–2126.

60 Thuéry, P. *Cryst. Growth Des*. **2011**, *11*, 2606–2620.

61 Thuéry, P. *Cryst. Growth Des*. **2011**, *11*, 3282–3294.

62 Thuéry, P. *Cryst. Growth Des*. **2012**, *12*, 499–507.

63 Thuéry, P.; Harrowfield, J. *CrystEngComm* **2015**, *17*, 4006–4018.

64 McKinnon, J. J.; Jayatilaka, D.; Spackman, M. A. *Chem. Commun.* **2007**, 3814–3816.

65 Spackman, M. A.; Jayatilaka, D. *CrystEngComm* **2009**, *11*, 19–32.

66 Spackman, M. A. *Phys. Scr.* **2013**, *87*, 048103 (12 pp).

67 Wolff, S. K.; Grimwood, D. J.; McKinnon, J. J.; Turner, M. J.; Jayatilaka, D.; Spackman, M. A. *CrystalExplorer*, University of Western Australia, 2012.

68 Groom, C. R.; Bruno, I. J.; Lightfoot, M. P.; Ward, S. C. The Cambridge Structural Database. *Acta Crystallogr., Sect. B* **2016**, *72*, 171–179.

69 Kaes, C.; Katz, A.; Hosseini, M. W. *Chem. Rev.* **2000**, *100*, 3553–3590.

70 Öhrström, L.; Larsson, K. Molecular-Based Materials – The Structural Network Approach, Elsevier, Amsterdam, 2005.

71 Harrowfield, J. M.; Maghaminia, S.; Soudi, A. A. *Inorg. Chem.* **2004**, *43*, 1810–1812.

72 Thuéry, P.; Harrowfield, J. *Cryst. Growth Des*. **2014**, *14*, 1314–1323.

73 Taylor, R.; Kennard, O. *J. Am. Chem. Soc*. **1982**, *104*, 5063–5070.

74 Desiraju, G. R. *Acc. Chem. Res*. **1991**, *24*, 290–296.

75 Desiraju, G. R. *Acc. Chem. Res*. **1996**, *29*, 441–449.

76 Harrowfield, J. M.; Shahverdizadeh, G.; Soudi, A. A. *Supramol. Chem.* **2003**, *15*, 367–373.

77 Knope, K. E.; de Lill, D. T.; Rowland, C. E.; Cantos, P. M.; de Bettencourt-Dias, A.; Cahill, C. L. *Inorg. Chem.* **2012**, *51*, 201–206.

78 Thangavelu, S. G.; Cahill, C. L. *Cryst. Growth Des*. **2016**, *16*, 42–50.

79 Brachmann, A.; Geipel, G.; Bernhard, G.; Nitsche, H. *Radiochim. Acta* **2002**, *90*, 147–153.

80 Thuéry, P.; Harrowfield, J. *Polyhedron* **2015**, *98*, 5–11.

81 Thuéry, P.; Masci, B.; Harrowfield, J. *Cryst. Growth Des*. **2013**, *13*, 3216–3224.

82 Thuéry, P.; Harrowfield, J. *Inorg. Chem.* **2015**, *54*, 6296–6305.

83 Zhang, Y.; Karatchevtseva, I.; Bhadbhade, M.; Tran, T. T.; Aharonovich, I.; Fanna, D. J.; Shepherd, N. D.; Lu, K.; Li, F.; Lumpkin, G. R. *J. Solid State Chem*. **2016**, *234*, 22–28.

84 Redmond, M. P.; Cornet, S. M.; Woodall, S. D.; Whittaker, D.; Collison, D.; Helliwell, M.; Natrajan, L. S. *Dalton Trans*. **2011**, *40*, 3914–3926.

85 Carter, K. P.; Kalaj, M.; Cahill, C. L. *Eur. J. Inorg. Chem*. **2016**, 126–137.

Table 1. Crystal Data and Structure Refinement Details

	1	2	3	4	5
chemical formula	$C_{54}H_{52}Ag_2N_{10}O_{18}U_2$	$C_{29}H_{36}N_3O_{12}PbU$	$C_9H_{13}AgO_{10}U$	$C_{42}H_{40}Ag_2N_6O_{16}U_2$	$C_{26}H_{15}AgN_2O_{10}U$
M (g mol^{-1})	1820.85	1063.83	627.09	1576.6	861.30
cryst syst	triclinic	triclinic	monoclinic	monoclinic	monoclinic
space group	$P\bar{1}$	$P\bar{1}$	$P2_1$	$P2_1/n$	$P2_1/c$
a (Å)	12.6023(6)	12.4437(8)	5.8163(3)	9.9284(4)	7.3661(2)
b (Å)	15.8090(13)	12.4791(7)	13.9064(7)	15.5092(11)	24.7771(10)
c (Å)	16.0831(12)	12.6490(6)	8.5949(3)	14.8738(10)	13.3875(5)
α (deg)	88.907(4)	106.682(3)	90	90	90
β (deg)	68.069(4)	104.890(3)	94.758(3)	91.299(4)	98.779(2)
γ (deg)	80.341(5)	109.876(3)	90	90	90
V (Å^3)	2926.9(4)	1626.65(18)	692.79(6)	2289.7(2)	2414.74(15)
Z	2	2	2	2	4
D_{calcd} (g cm^{-3})	2.066	2.172	3.006	2.287	2.369
μ(Mo Kα) (mm^{-1})	6.256	10.206	13.134	7.972	7.576
F(000)	1736	1002	572	1480	1616
reflns collcd	157880	90085	43704	73107	80298
indep reflns	11116	8397	4239	4331	6212
obsd reflns [$I > 2\sigma(I)$]	8559	6756	4200	3845	5270
R_{int}	0.098	0.060	0.016	0.038	0.029
params refined	775	415	190	309	361
R_1	0.036	0.030	0.017	0.059	0.024
wR_2	0.076	0.073	0.041	0.166	0.056
S	0.990	1.006	1.047	1.200	0.995
$\Delta\rho_{min}$ (e Å^{-3})	–2.28	–2.00	–1.17	–3.09	–1.13
$\Delta\rho_{max}$ (e Å^{-3})	0.87	1.92	0.71	3.01	0.72

	6	7	8	9	10
chemical formula	$C_{36}H_{22}N_4O_{10}PbU$	$C_{23.5}H_{25.5}N_{1.5}O_{16.5}U_2$	$C_{33}H_{33}AgN_6O_{14}U$	$C_{32}H_{22}N_6O_6U$	$C_{39.5}H_{24.5}N_{6.5}O_{15}Pb_2U$
M (g mol^{-1})	1115.79	1069.01	1083.55	824.58	1482.56
cryst syst	monoclinic	monoclinic	triclinic	triclinic	triclinic
space group	$C2/c$	$P2_1/c$	$P\bar{1}$	$P\bar{1}$	$P\bar{1}$
a (Å)	12.6793(11)	15.8274(10)	12.7924(7)	7.5068(5)	9.5004(2)
b (Å)	22.8373(11)	9.6221(6)	12.8060(7)	9.9888(3)	13.9275(6)
c (Å)	11.8893(10)	20.2022(7)	13.3730(5)	19.9323(13)	16.1073(7)
α (deg)	90	90	62.759(4)	95.104(4)	107.195(2)
β (deg)	111.830(4)	96.855(4)	64.182(4)	90.958(3)	99.118(3)
γ (deg)	90	90	76.753(4)	109.215(3)	101.459(3)
V (Å^3)	3195.8(4)	3054.7(3)	1752.14(17)	1404.06(14)	1940.99(13)
Z	4	4	2	2	2
D_{calcd} (g cm^{-3})	2.319	2.325	2.054	1.950	2.537
μ(Mo Kα) (mm^{-1})	10.393	10.666	5.254	5.839	12.899
F(000)	2080	1972	1048	792	1366
reflns collcd	52424	110892	80748	73552	109389
indep reflns	3041	5796	6655	5313	10030
obsd reflns [$I > 2\sigma(I)$]	2623	4732	6031	4896	8325
R_{int}	0.055	0.035	0.047	0.042	0.064
params refined	237	426	496	407	586
R_1	0.028	0.038	0.039	0.040	0.025
wR_2	0.062	0.101	0.102	0.106	0.051
S	1.035	1.068	1.065	1.225	0.977
$\Delta\rho_{min}$ (e Å^{-3})	–1.46	–1.75	–1.85	–1.72	–1.91
$\Delta\rho_{max}$ (e Å^{-3})	1.55	3.20	2.99	2.45	1.01

Figure Captions

Figure 1. Top: View of complex **1**. Displacement ellipsoids are drawn at the 50% probability level. Symmetry codes: i = $x - 1$, y, z; j = $x + 1$, y, z. Middle: View of the packing with the uranium coordination polyhedra colored yellow and silver atoms shown as blue spheres. Bottom: The columnar arrangement of counter-ions. Hydrogen atoms are omitted in all views.

Figure 2. Top left: View of complex **2**. Displacement ellipsoids are drawn at the 50% probability level. Carbon-bound hydrogen atoms are omitted and hydrogen bonds are shown as dashed lines. Symmetry codes: i = x, $y - 1$, z; j = x, $y + 1$, z; k = $1 - x$, $2 - y$, $2 - z$; l = $-x$, $-y$, $2 - z$. Top right: View of the 1D polymer. Bottom left: View of one chain down its axis. Bottom right: View of the packing with chains viewed end-on. Lattice water molecules and hydrogen atoms are omitted; uranium coordination polyhedra are colored yellow and lead atoms are shown as green spheres in the last three views.

Figure 3. Top left: View of complex **3**. Displacement ellipsoids are drawn at the 50% probability level and carbon-bound hydrogen atoms are omitted. Symmetry codes: i = $x - 1$, y, $z - 1$; j = $-x$, $y - 1/2$, $2 - z$; k = x, y, $z - 1$; l = $x + 1$, y, $z + 1$; m = x, y, $z + 1$; n = $-x$, $y + 1/2$, $2 - z$. Top right: Hirshfeld surface mapped with d_{norm} showing silver oxo bonding. Bottom: Two views of the 3D framework with the uranium coordination polyhedra colored yellow, silver atoms shown as blue spheres, and hydrogen atoms omitted.

Figure 4. Top: View of complex **4**. Displacement ellipsoids are drawn at the 50% probability level. Symmetry codes: i = $x + 1, y, z$; j = $x + 1/2, 3/2 – y, z + 1/2$; k = $x – 1, y, z$; l = $x – 1/2, 3/2 – y, z – 1/2$; m = $2 – x, 1 – y, 1 – z$. Middle: View of the 2D network with the uranium coordination polyhedra colored yellow and silver atoms shown as blue spheres; four counterions only are represented for clarity. Bottom: Packing with sheets viewed edge-on. Hydrogen atoms are omitted in all views.

Figure 5. Top left: View of complex **5**. Displacement ellipsoids are drawn at the 50% probability level. Carbon-bound hydrogen atoms are omitted and the hydrogen bond is shown as a dashed line. Symmetry codes: i = $x + 1, y, z$; j = $1 – x, y + 1/2, 3/2 – z$; k = $2 – x, y + 1/2, 3/2 – z$; l = $x – 1, y, z$; m = $1 – x, y – 1/2, 3/2 – z$; n = $2 – x, y – 1/2, 3/2 – z$. Top right: View of the 2D assembly built by uranyl cations and ligands alone. Bottom left: View of the 2D assembly including silver(I) and 4,4′-bipyH$^+$ cations. Bottom right: Packing with sheets viewed edge-on. Uranium coordination polyhedra are colored yellow, silver atoms are blue spheres, and hydrogen atoms are omitted in the last three views.

Figure 6. Top: View of complex **6**. Displacement ellipsoids are drawn at the 50% probability level. Symmetry codes: i = $1 – x, 1 – y, 1 – z$; j = $1 – x, y, 3/2 – z$; k = $x, 1 – y, z – 1/2$; l = $–x, y, 3/2 – z$; m = $x – 1, y, z$. Middle: View of the 2D assembly. Bottom: Packing with sheets viewed edge-on. Uranium coordination polyhedra are colored yellow and lead atoms are green spheres. Hydrogen atoms are omitted in all views.

Figure 7. Top left: View of complex **7**. Displacement ellipsoids are drawn at the 50% probability level. The solvent molecules and carbon-bound hydrogen atoms are omitted, and the hydrogen

bond is shown as a dashed line. Symmetry codes: i = 1 – *x*, 1 – *y*, 1 – *z*; j = 1 – *x*, *y* + 1/2, 3/2 – *z*; k = *x* – 1, *y*, *z*; l = 1 – *x*, *y* – 1/2, 3/2 – *z*; m = *x* + 1, *y*, *z*. Top right and bottom left: Two views of the 3D framework with the uranium coordination polyhedra colored yellow; solvent molecules and hydrogen atoms are omitted. Bottom right: Nodal representation of the framework showing the location of the NMP molecules in the channels parallel to the *a* axis (yellow: uranium, red: oxygen, blue: tetracarboxylate ligand, dark red: NMP molecules).

Figure 8. Top left: View of complex **8**. Displacement ellipsoids are drawn at the 30% probability level. The solvent molecules and carbon-bound hydrogen atoms are omitted. Symmetry codes: i = *x* – 1, *y*, *z*; j = 1 – *x*, 1 – *y*, 1 – *z*; k = *x* + 1, *y*, *z*. Top right: Hirshfeld surface mapped with d_{norm} showing the hydrogen bonding interactions. Bottom left: View of the 1D polymer (double chain with oxo bonding). Bottom right: View of the packing with the chains viewed end-on. Uranium coordination polyhedra are colored yellow and silver atoms are shown as blue spheres. Solvent molecules and hydrogen atoms are omitted.

Figure 9. Top left: View of complex **9**. Displacement ellipsoids are drawn at the 50% probability level. Top right: Hirshfeld surface mapped with d_{norm} showing the location of CH···O interactions as red dots. Bottom: View of the packing with uranium coordination polyhedra colored yellow. Hydrogen atoms are omitted in both views.

Figure 10. Top: View of complex **10**. Displacement ellipsoids are drawn at the 50% probability level. Symmetry codes: i = 1 – *x*, 1 – *y*, 1 – *z*; j = 2 – *x*, 2 – *y*, 2 – *z*. Bottom: View of the packing of chains with the uranium coordination polyhedra colored yellow and lead atoms shown as green

spheres. In both views, solvent molecules and hydrogen atoms are omitted, and formate anions only are shown in the disordered parts.

Figure 11. Solid state emission spectra recorded with an excitation wavelength of 420 nm.

Figure 1

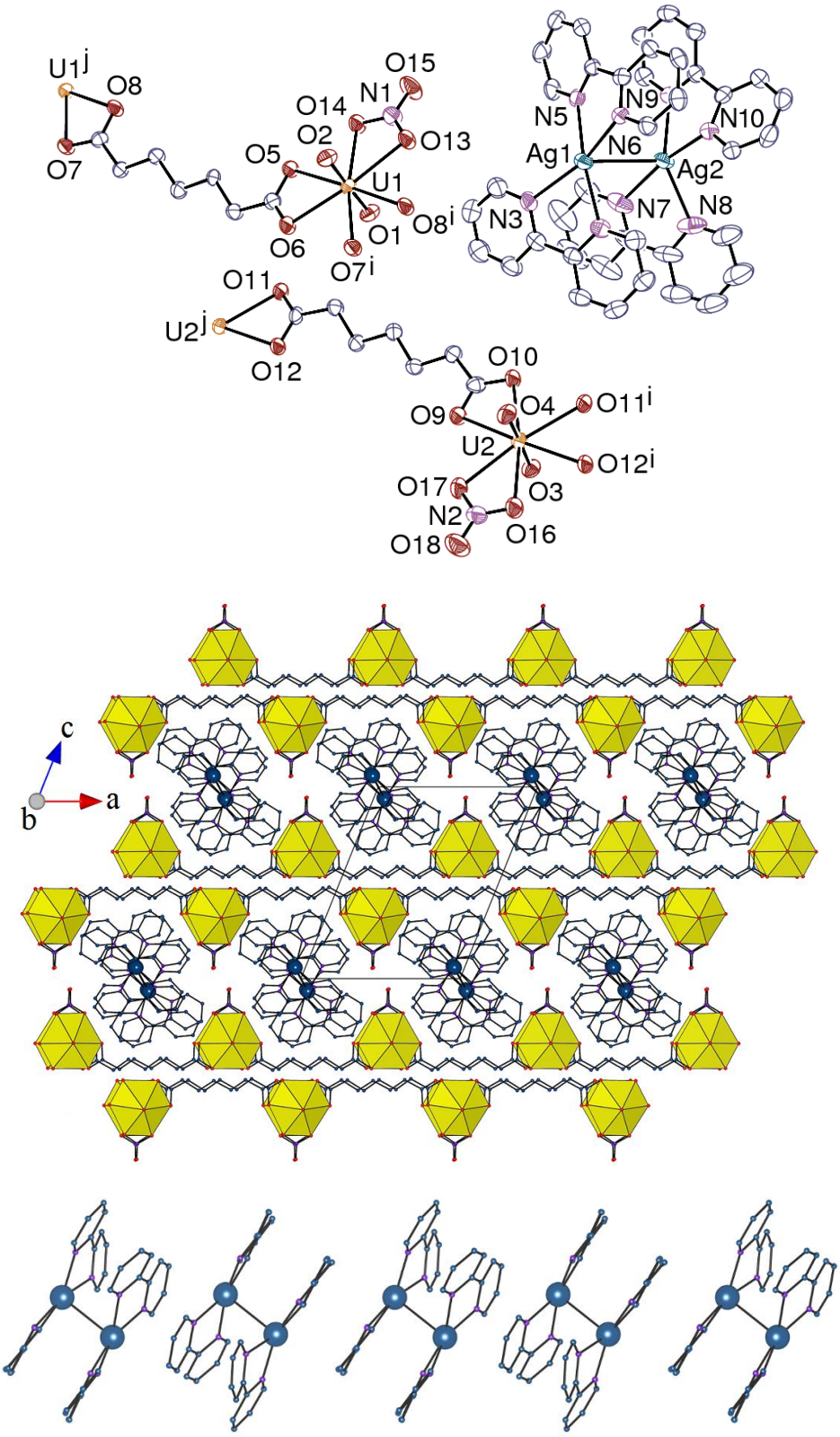
U1j
O8
O7
O15
N1
O14
O2
O13
O5
U1
O6
O1
O8i
O7i
N5
N9
N10
Ag1
N6
Ag2
N3
N7
N8
O11
U2j
O12
O10
O9
O4
O11i
U2
O12i
O17
O3
N2
O16
O18
c
a
b

Figure 2

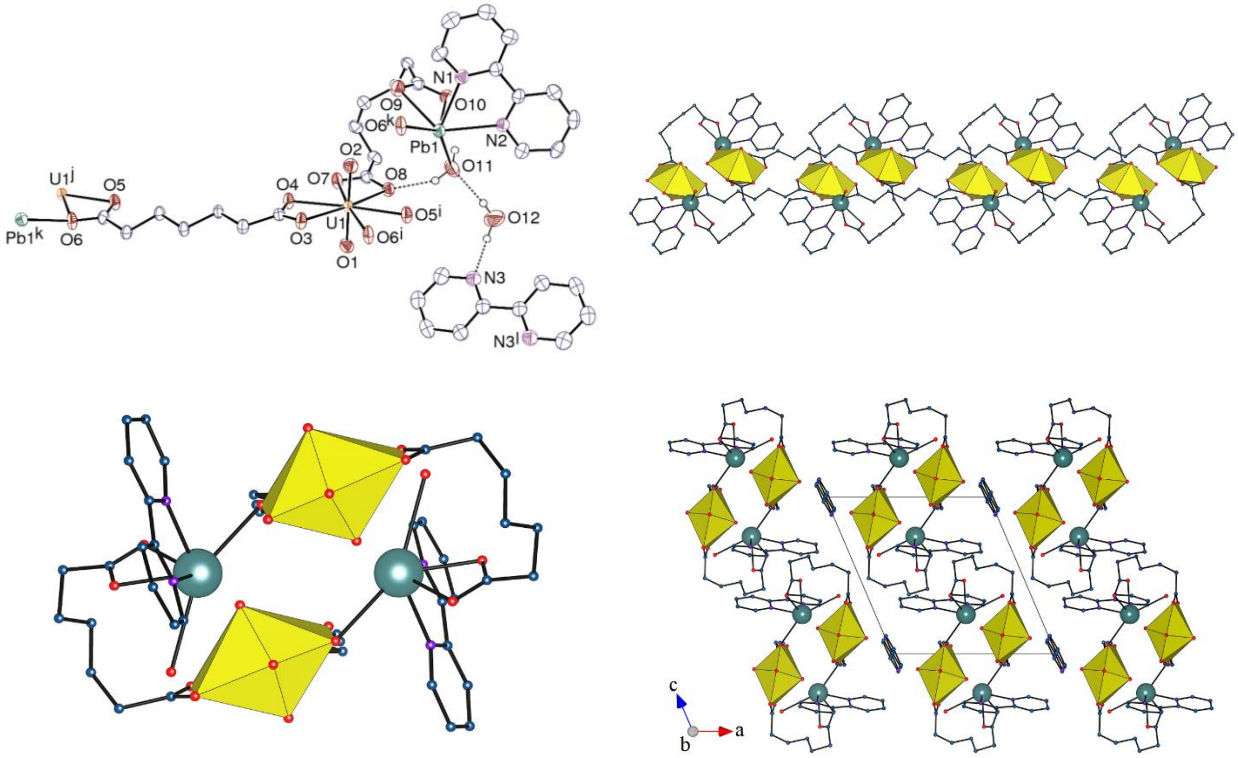
N1
O9
O10
O6k
Pb1
N2
O2
O11
U1i
O5
O4
O7
O8
O5i
O12
Pb1k
O6
O3
U1
O6i
O1
N3
N3l
c
a
b

Figure 3

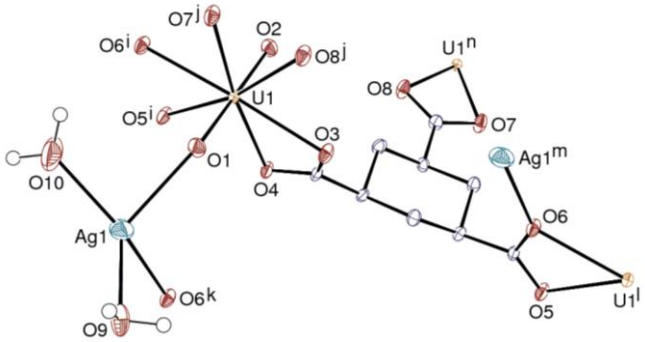
O7i
O2
O6i
O8j
U1n
U1
O8
O5i
O7
O3
Ag1m
O1
O10
O4
O6
Ag1
O6k
O5
U1l
O9

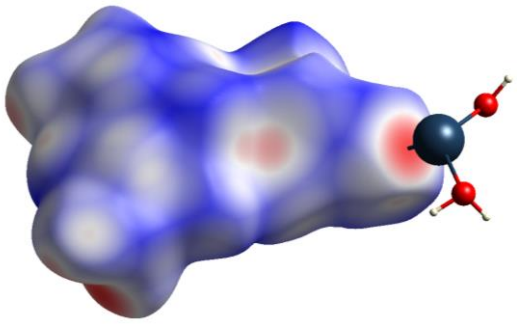

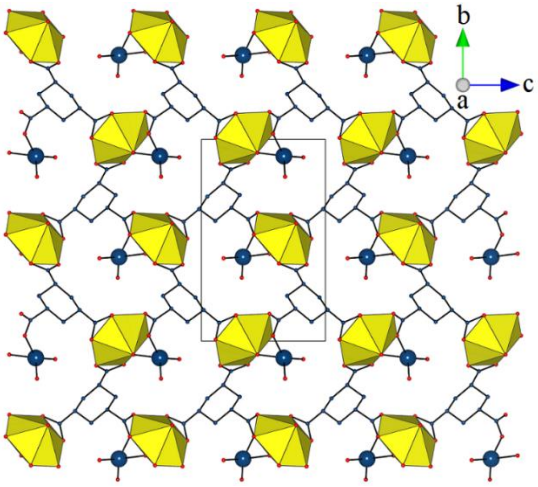
b
c
a

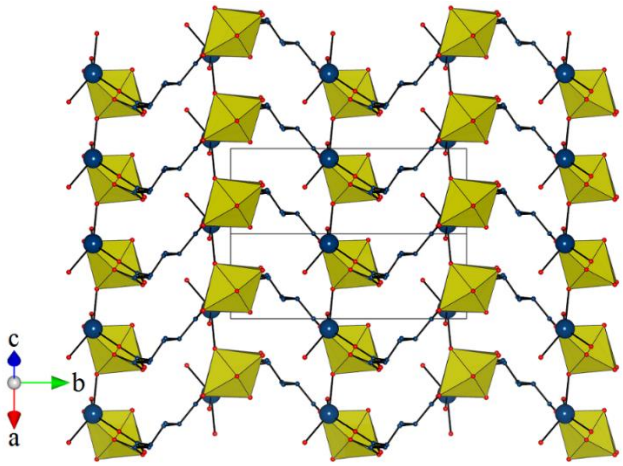
c
b
a

Figure 4

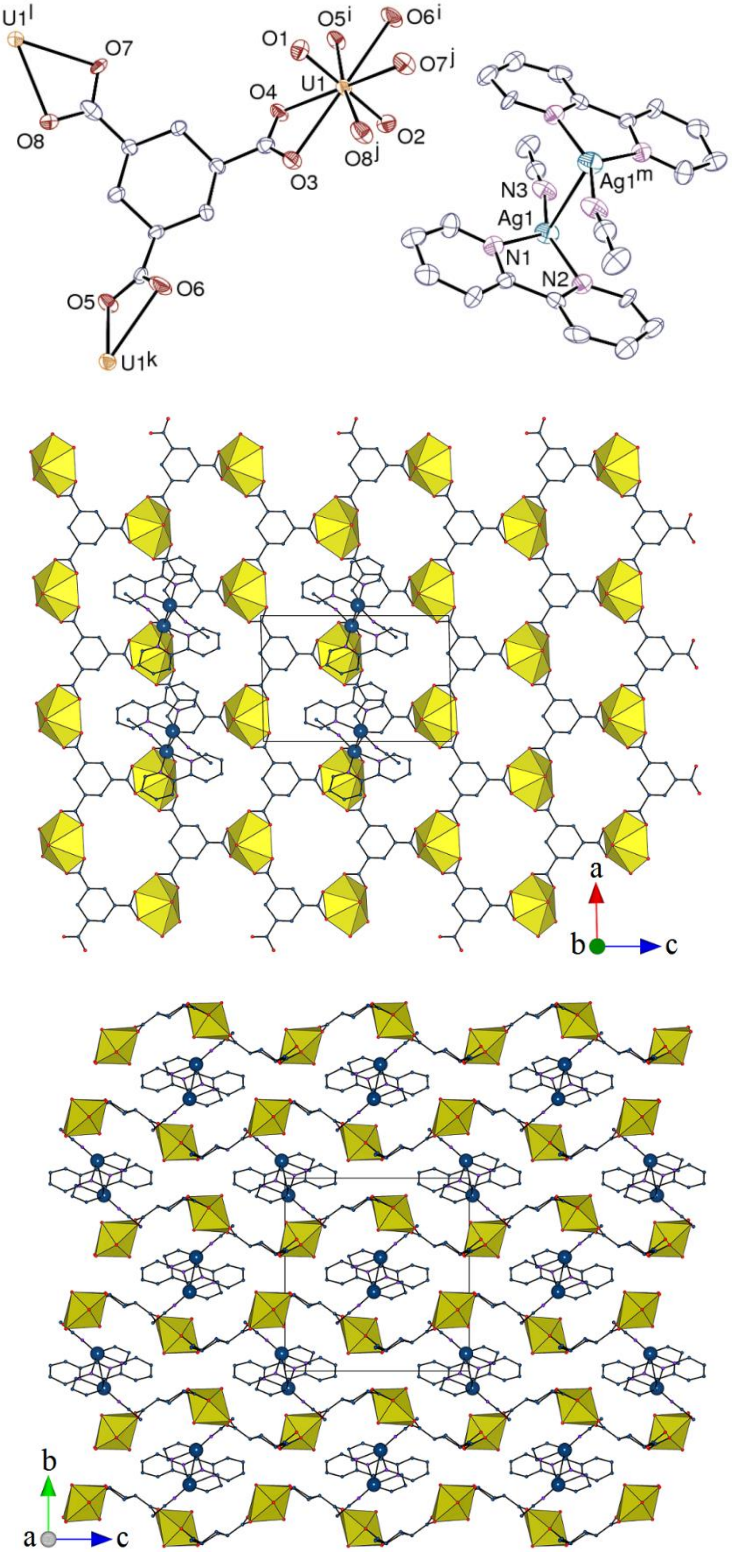
U1l
O7
O8
O1
O5i
O6i
O7j
U1
O4
O2
O8j
O3
N3
Ag1m
Ag1
N1
N2
O5
O6
U1k
a
b
c
b
a
c

Figure 5

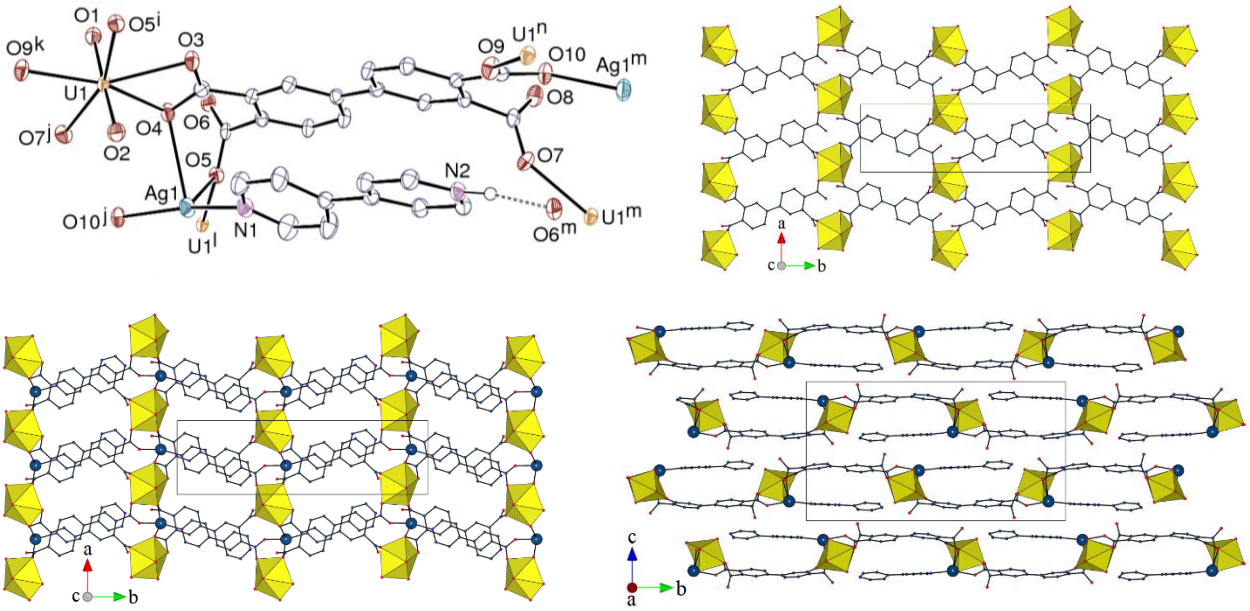
O1
O5i
O9k
O3
U1
O9
U1n
O10
Ag1m
O8
O7i
O4
O6
O2
O5
O7
N2
Ag1
O10j
N1
U1l
O6m
U1m
a
c
b

Figure 6

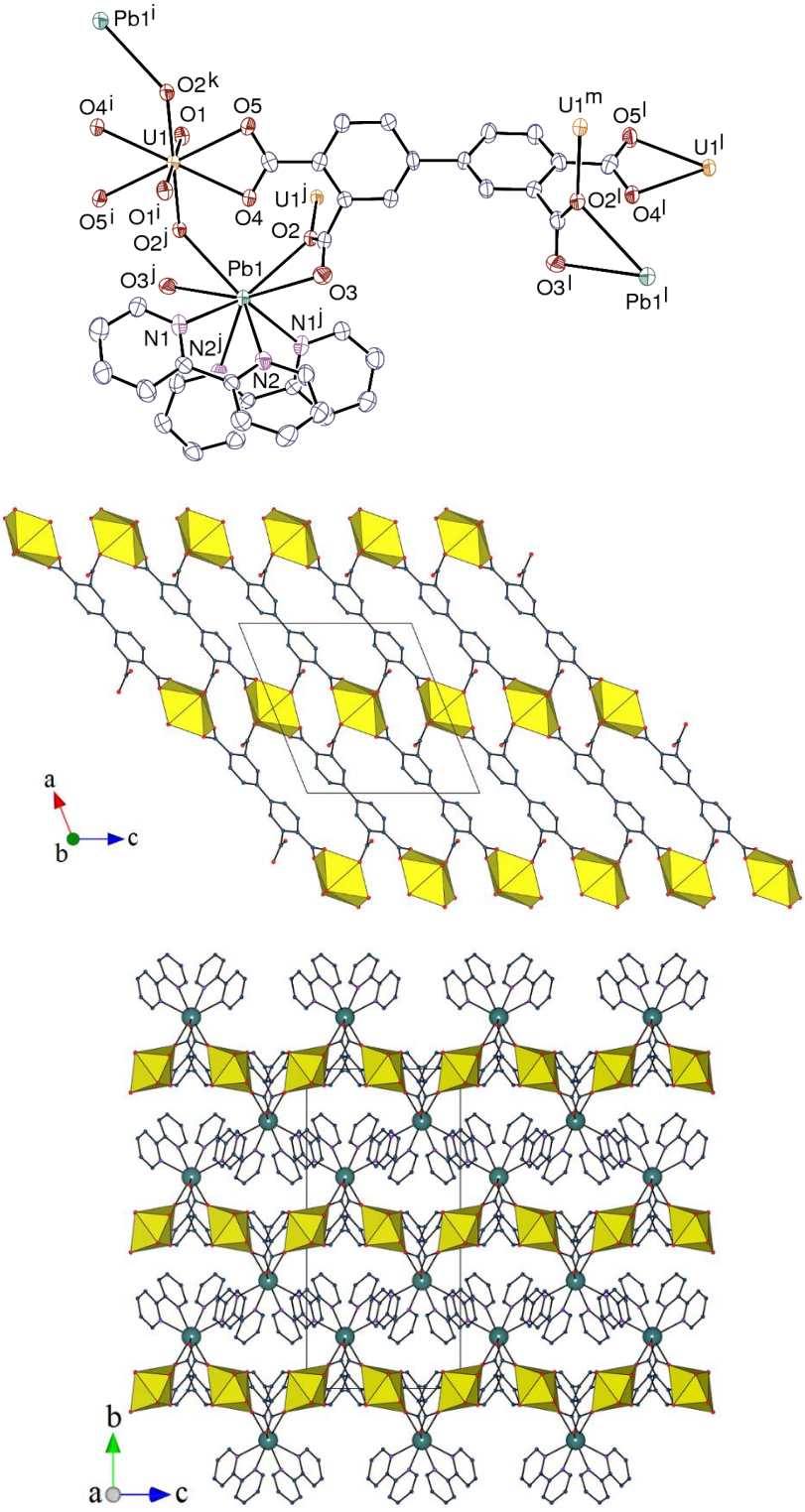
Pb1i
O2k
O4i
O1
O5
U1
U1m
O5l
U1l
O5i
O1i
O4
U1j
O2
O2l
O4l
O2j
Pb1
O3j
O3
O3l
Pb1l
N1
N1j
N2j
N2
a
b
c
b
a
c

Figure 7

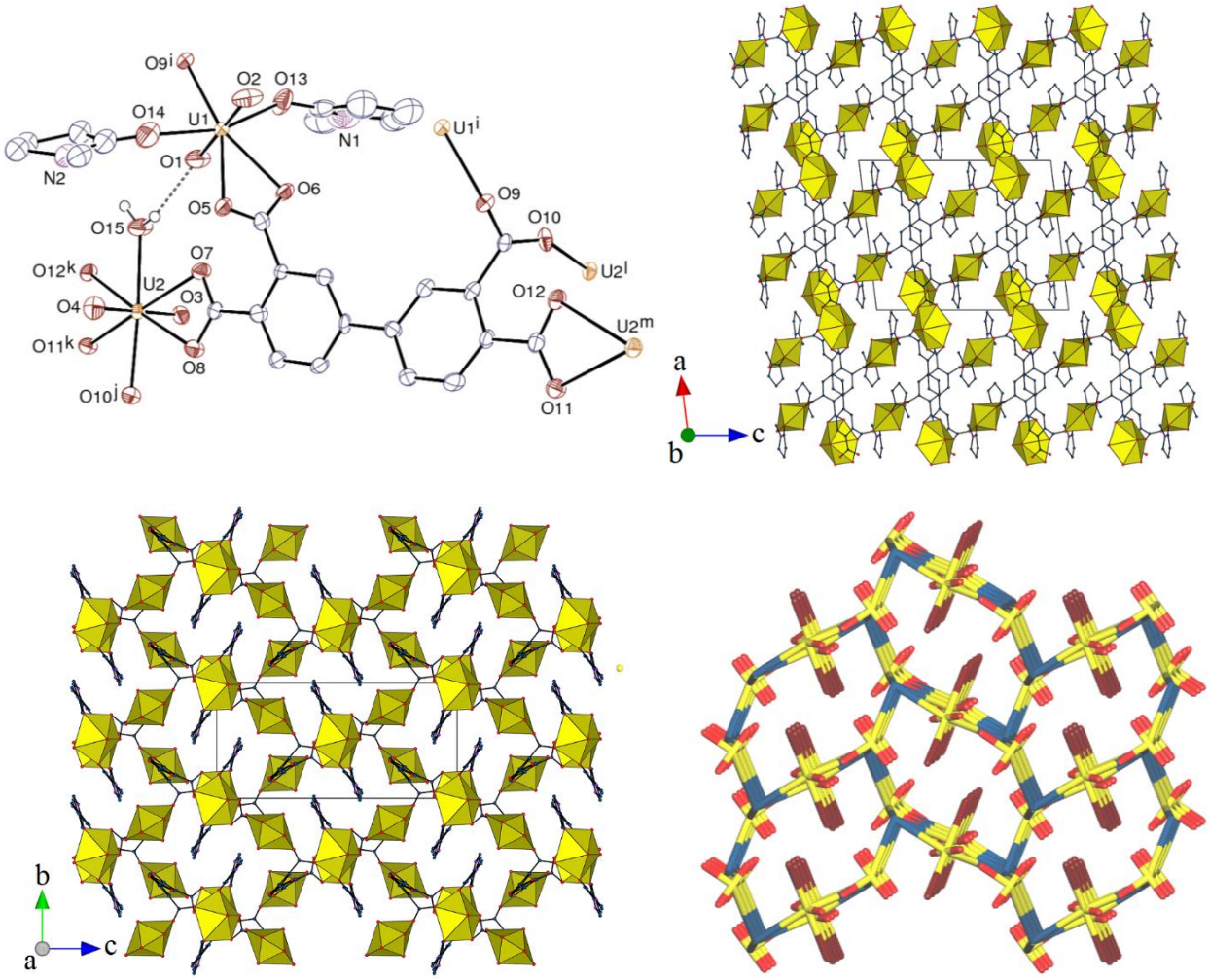
O9i
O2
O13
O14
U1
N1
U1i
N2
O1
O6
O9
O5
O10
O15
O7
U2l
O12k
U2
O12
O4
O3
U2m
O11k
O8
O10i
O11
a
b
c
b
a
c

Figure 8

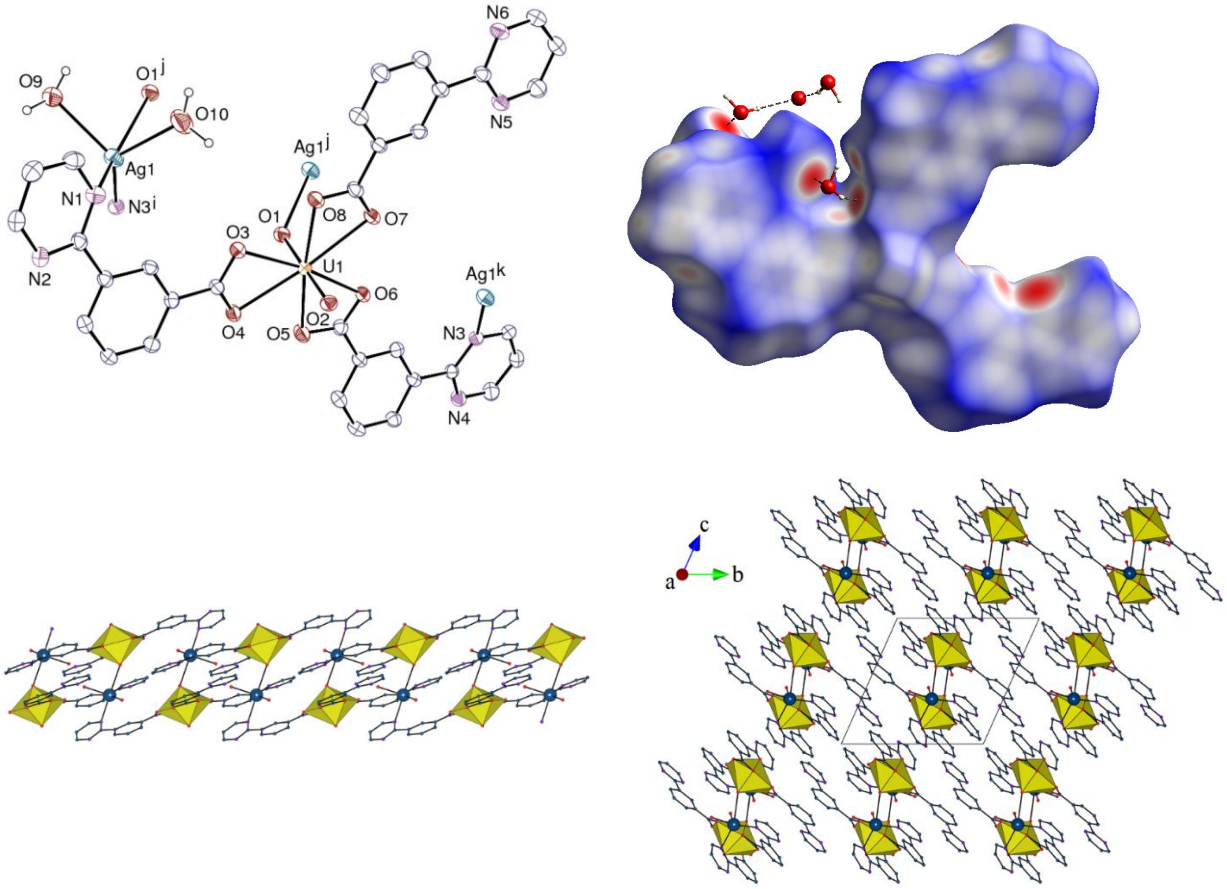
O9
O1j
O10
Ag1
N1
N3i
N2
O3
O1
Ag1j
O8
O7
N6
N5
U1
O6
O4
O5
O2
Ag1k
N3
N4
c
a
b

Figure 9

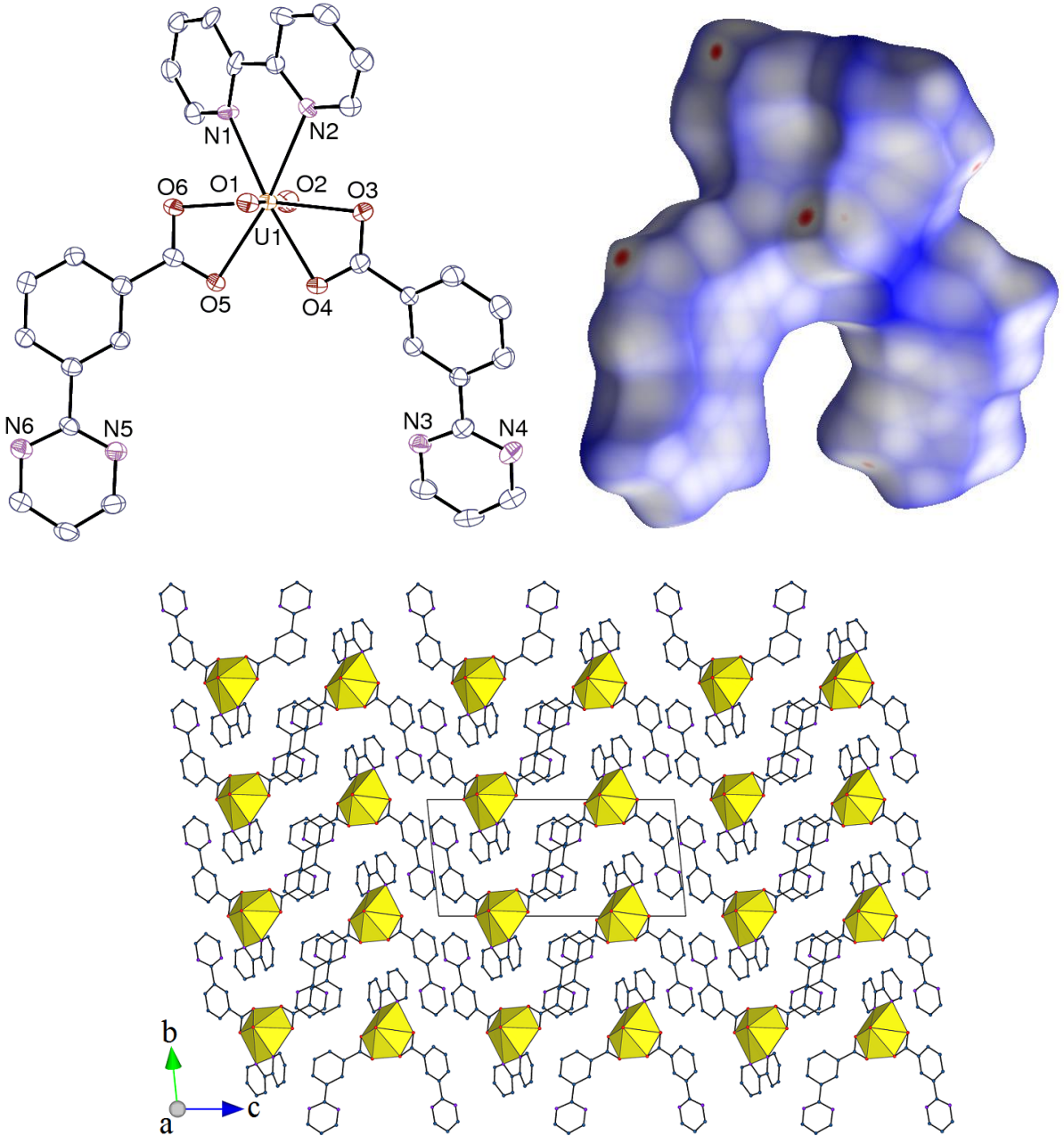

Figure 10

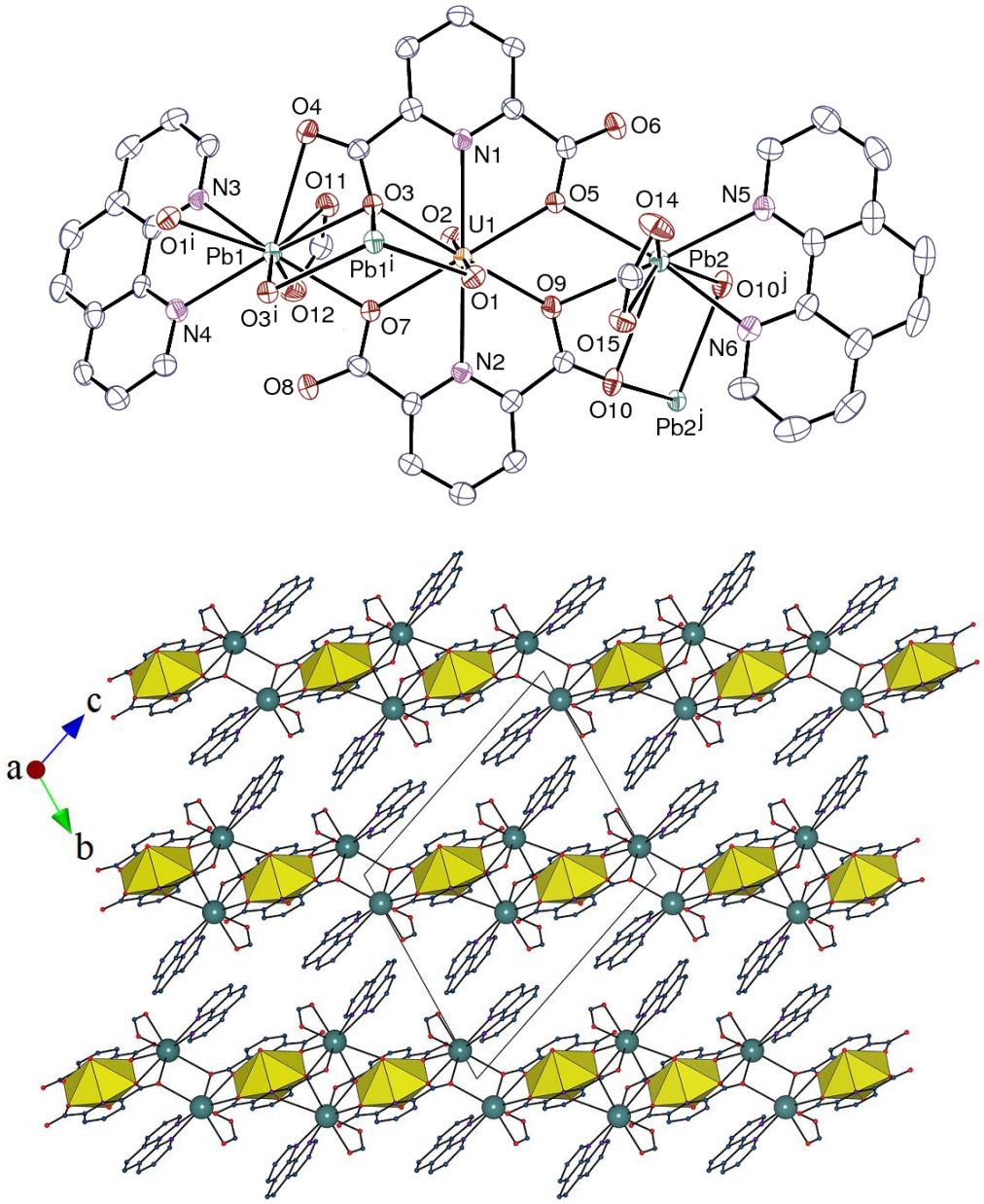
O4
O6
N1
N3
O11
O3
O2
U1
O5
O14
N5
O1i
Pb1
Pb1i
O9
Pb2
O10j
O3i
O12
O7
O1
N4
O15
N6
N2
O8
O10
Pb2j
c
a
b

Figure 11

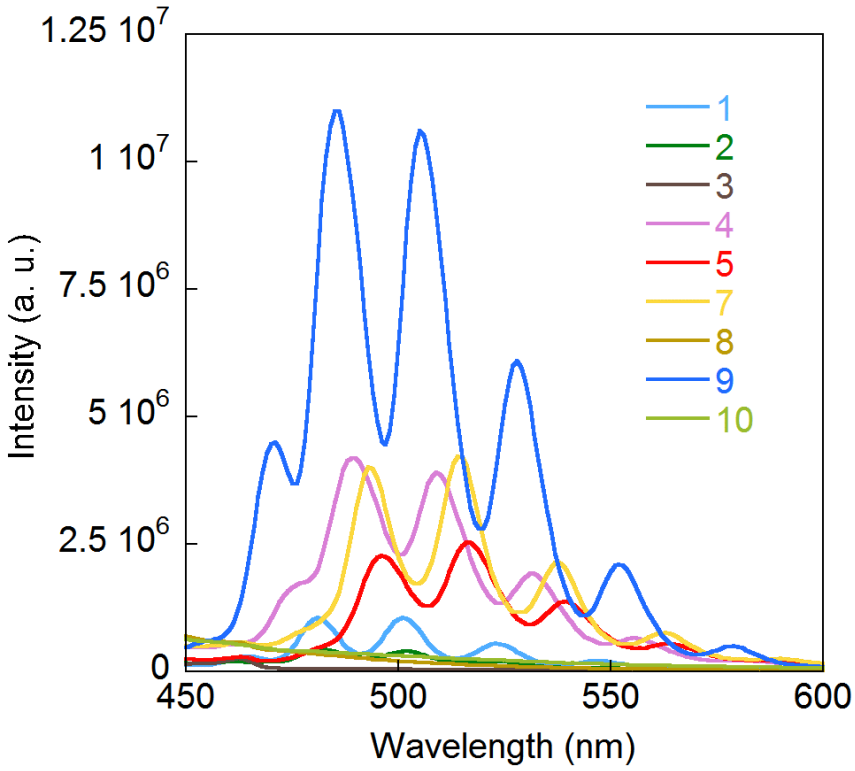
1.25 10^7
1 10^7
7.5 10^6
5 10^6
2.5 10^6
0
Intensity (a. u.)
450
500
550
600
Wavelength (nm)
1
2
3
4
5
7
8
9
10

For Table of Contents Use Only

Ag^{I} and Pb^{II} as Additional Assembling Cations in Uranyl Coordination Polymers and Frameworks

Pierre Thuéry and Jack Harrowfield

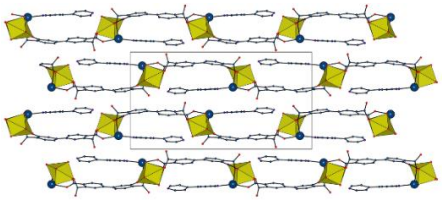

A series of eight heterometallic complexes with uranyl and either silver(I) or lead(II) cations, and five different carboxylate ligands offering a broad range of structural possibilities, displays various novel modes of association (including Ag^{I} or Pb^{II} oxo-bonding to uranyl in some cases) depending on the metallic cation and the nature of the ligand.